Announcement

- This course is now open for Student Opinion Survey submissions
- Please go to https://www.odu.edu/technology-services/student-opinion-survey and fill out the survey – I very much want to know your (anonymous) opinion and suggestions.
- If at least 50% (3 people) participate, I will offer an extra credit problem on the Final Exam (Thursday 12/11 12:30 – 15:30 in the same room)

Collective Phenomena

- Giant resonances
- Deformation, high spin
- Squeezed nuclear matter
- Relativistic Heavy Ion Collisions

Giant Dipole Resonances

(from Povh et al.)

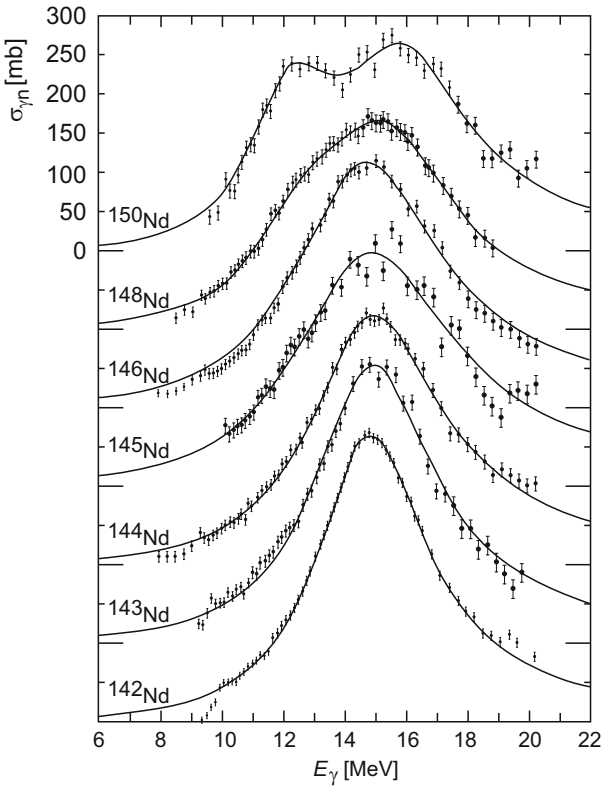

Fig. 19.3 Cross-section for γ-induced emission of neutrons in neodymium isotopes [2]. The curves have been shifted vertically for the sake of clarity. Neodymium isotopes progress from being spherically symmetric to being deformed nuclei. The giant resonance of the spherically symmetric ^{142}Nd nucleus is narrow, while that of the deformed ^{150}Nd nucleus shows a double peak

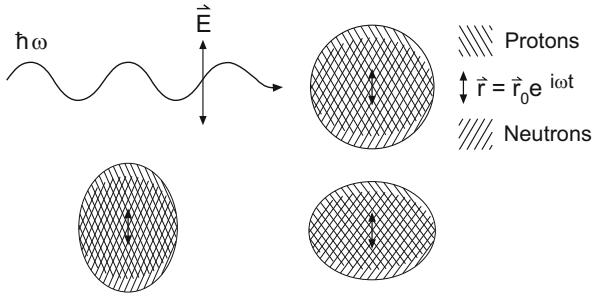

Fig. 19.4 The giant dipole resonance as oscillations of the protons and neutrons against each other. In deformed nuclei *(below)* two oscillation modes are available

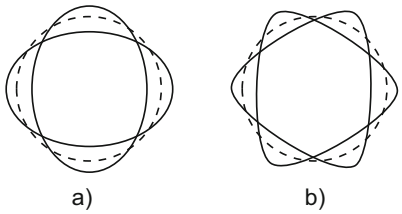

Fig. 19.7 (**a**) Quadrupole vibrations; (**b**) Octupole vibrations

Rotational States

(from Povh et al.)

Rotational energy in classical mechanics depends upon the angular momentum $\boldsymbol{J}$ and the moment of inertia Θ:

$$E_{\text{rot}} = \frac{|\boldsymbol{J}_{\text{rot}}|^2}{2\Theta} \,. \tag{19.42}$$

In quantum mechanics rotation is described by a Hamiltonian operator

$$\mathcal{H}_{\text{rot}} = \frac{\boldsymbol{J}^2}{2\Theta} \,. \tag{19.43}$$

In such a quantum mechanical system the rotation must be perpendicular to the symmetry axis. The eigenstates of the angular momentum operator $\boldsymbol{J}$ are the spherical harmonic functions Y_J^m, which describe the angular distribution of the wave function. The associated eigenvalues are:

$$E_J = J(J+1)\frac{\hbar^2}{2\Theta} \,. \tag{19.44}$$

The gaps between successive states increase linearly because of $E_{J+1} - E_J = 2(J+1)\hbar^2/2\Theta$. This is typical of rotating states. Only even values of J are attainable, for reasons of symmetry, for those nuclei which have $J^P = 0^+$ in the ground state. The moment of inertia Θ can be found from the spins and excitation energies.

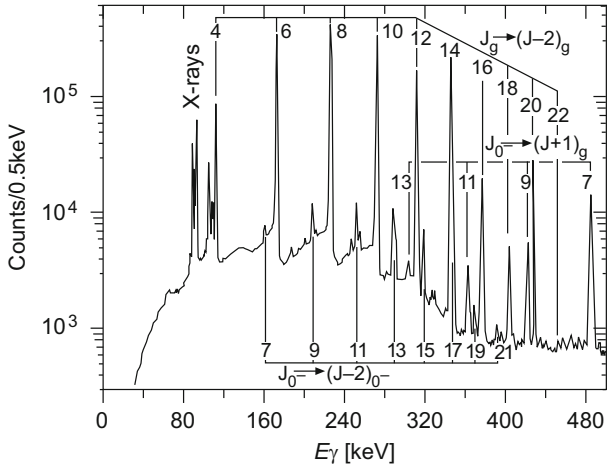

Fig. 19.10 Photon spectrum of a Coulomb excited ^{232}Th nucleus. Three series of matching lines may be seen. The strongest lines correspond to transitions in the ground state rotational band $J_g \rightarrow (J-2)_g$. The other two bands are strongly suppressed and are the results of excited states (cf. Fig. 19.12) [8]

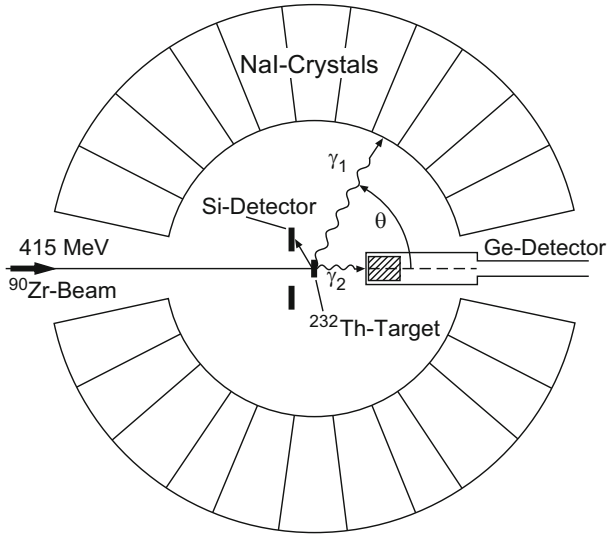

Fig. 19.11 Experimental apparatus for investigating Coulomb excitation in heavy ion collisions. In the example shown a ^{90}Zr beam hits a ^{232}Th target. The backwardly scattered Zr projectiles are detected in a silicon detector. A germanium detector, with which the γ cascades inside the rotational bands can be finely resolved, gives a precise measurement of the γ spectrum. These photons are additionally measured by a crystal ball of NaI crystals with a poorer resolution. A coincidence condition between the silicon detector and the NaI crystals can be used to single out an energy window inside which one may study the nuclear rotational states with the germanium detector (From [8])

The Structure of Matter

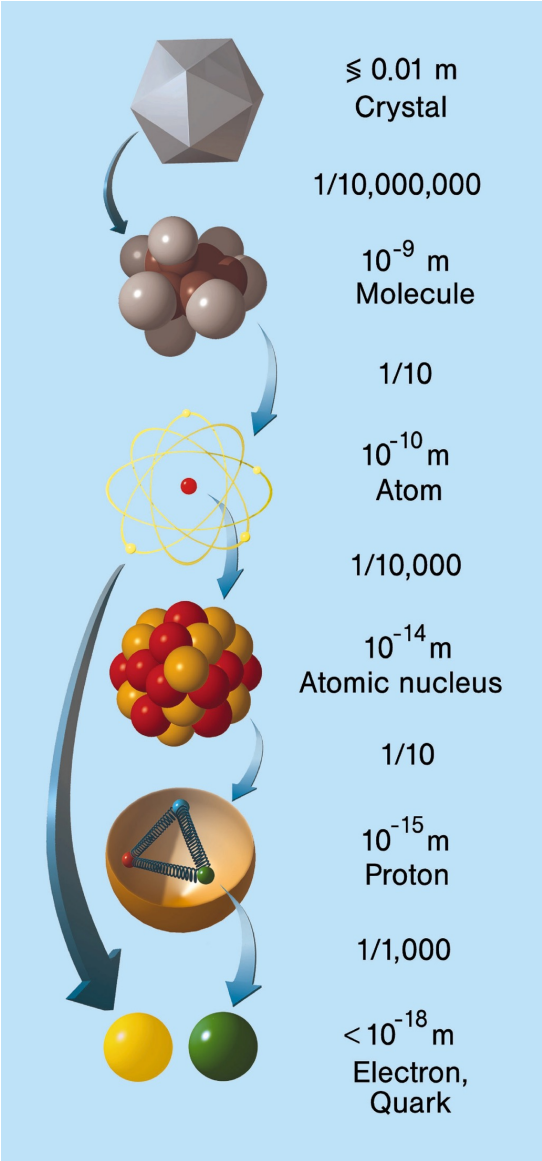

- What **nuclei** is the Universe made off?
- What nuclei where there in the beginning (right after the big bang)?
- When and how did nuclei important for life form?
- Where do heavy nuclei come from?

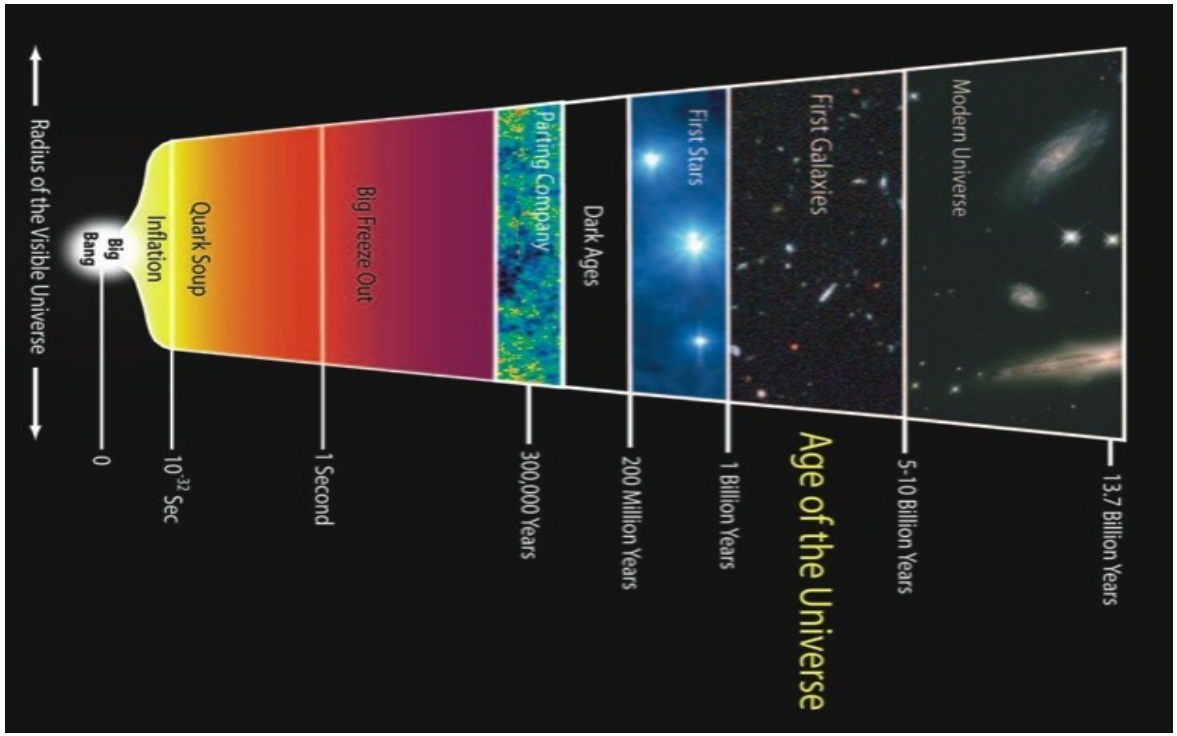

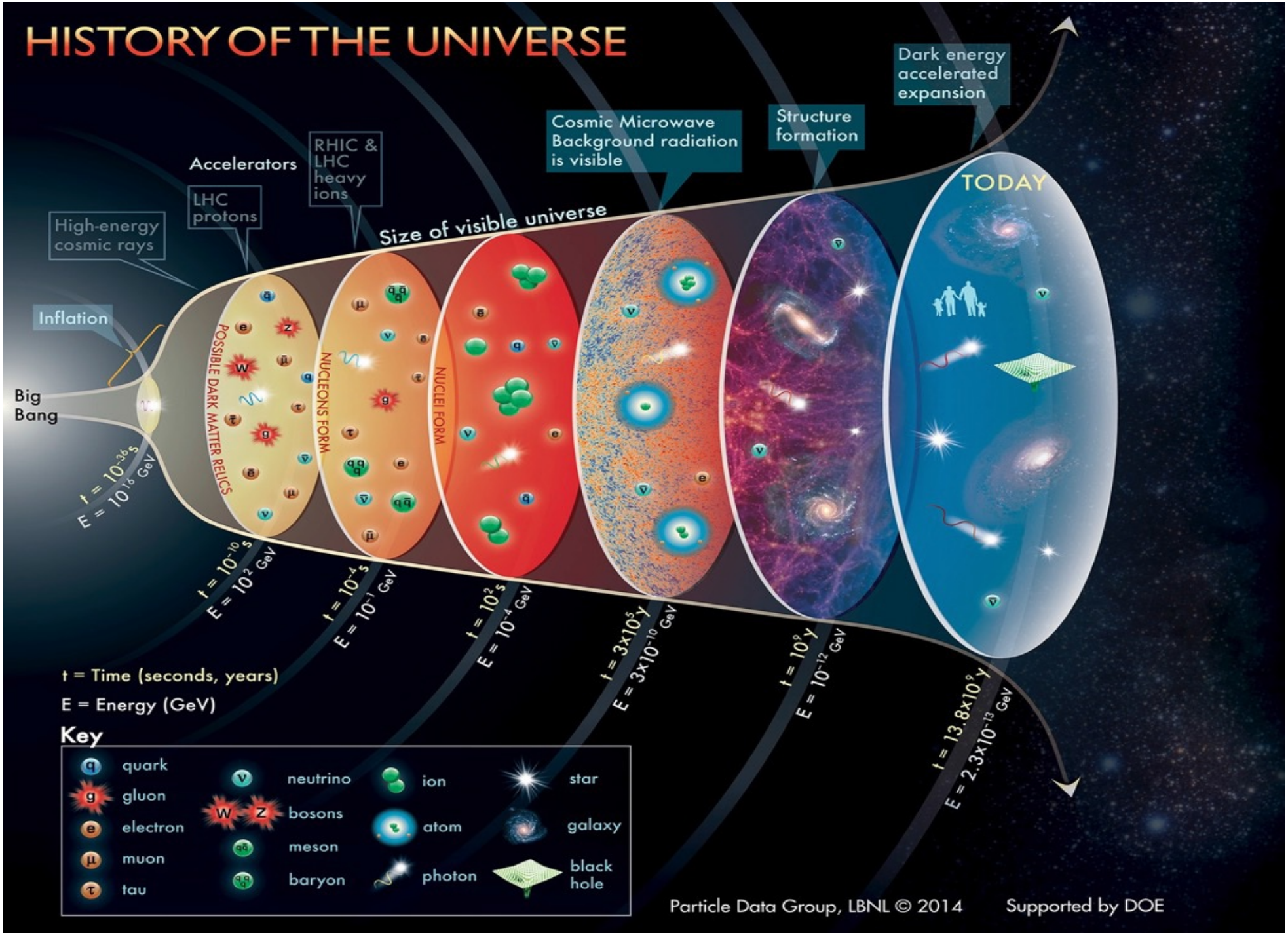
HISTORY OF THE UNIVERSE
Dark energy accelerated expansion
Structure formation
Cosmic Microwave Background radiation is visible
Accelerators
RHIC & LHC heavy ions
LHC protons
High-energy cosmic rays
Size of visible universe
TODAY
Inflation
Big Bang
POSSIBLE DARK MATTER RELICS
NUCLEONS FORM
NUCLEI FORM
t = 10^-36 s
E = 10^16 GeV
t = 10^-10 s
E = 10^2 GeV
t = 10^-4 s
E = 10^-1 GeV
t = 10^2 s
E = 10^-4 GeV
t = 3x10^5 y
E = 3x10^-10 GeV
t = 10^9 y
E = 10^-12 GeV
t = 13.8x10^9 y
E = 2.3x10^-13 GeV
t = Time (seconds, years)
E = Energy (GeV)
Key
quark
gluon
electron
muon
tau
neutrino
bosons
meson
baryon
ion
atom
photon
star
galaxy
black hole
Particle Data Group, LBNL © 2014
Supported by DOE

RHIC Physics: The Quark Gluon Plasma and The Color Glass Condensate: 4 Lectures*

Larry McLerran

Physics Department PO Box 5000 Brookhaven National Laboratory Upton, NY 11973 USA

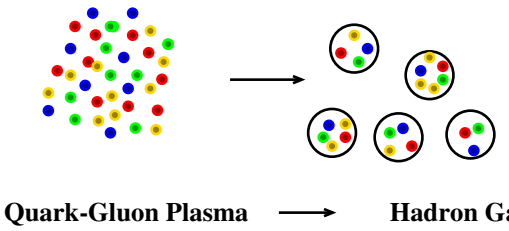

Figure 1: As the energy density is decreased, the Quark Gluon Plasma condenses into a low density gas of hadrons. Quarks are red, green or blue and gluons are yellow.

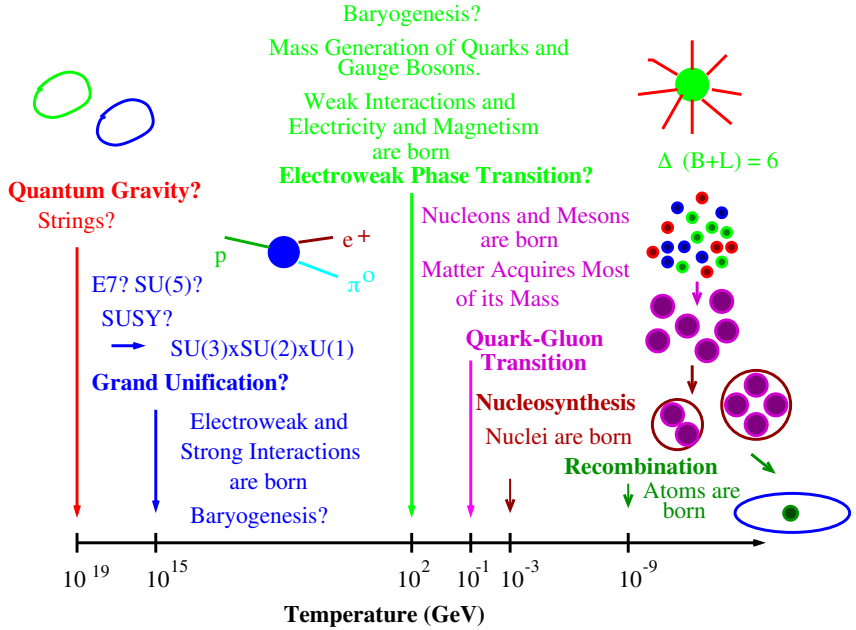

Figure 2: The various forms of matter, and the types of physics which are probed during the big bang.

Phase Diagram for Baryonic Matter

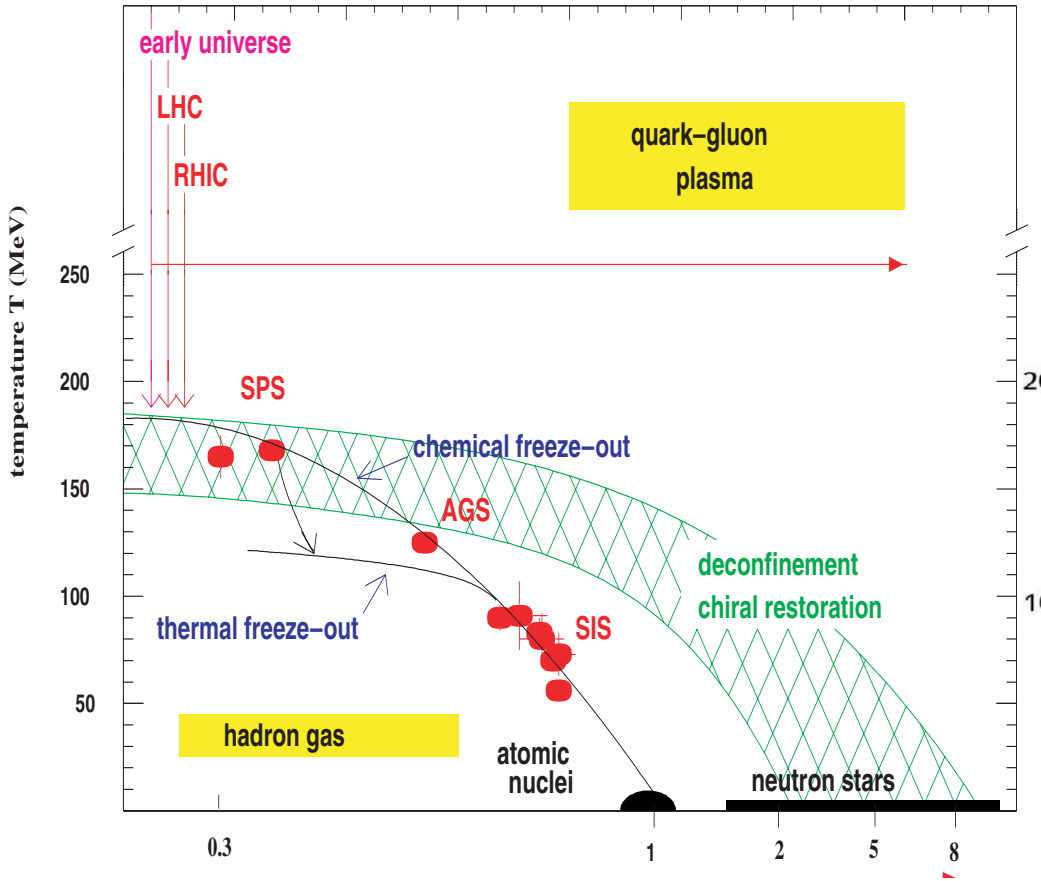

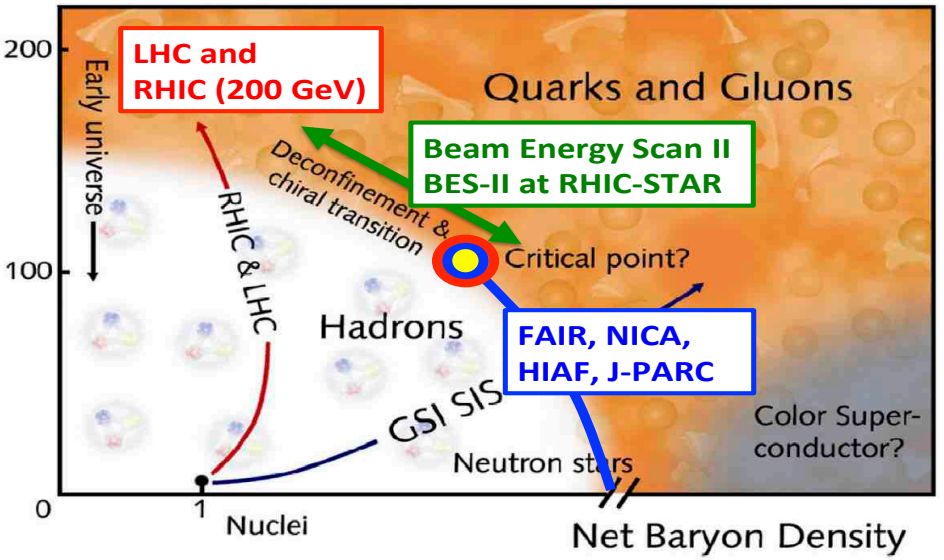

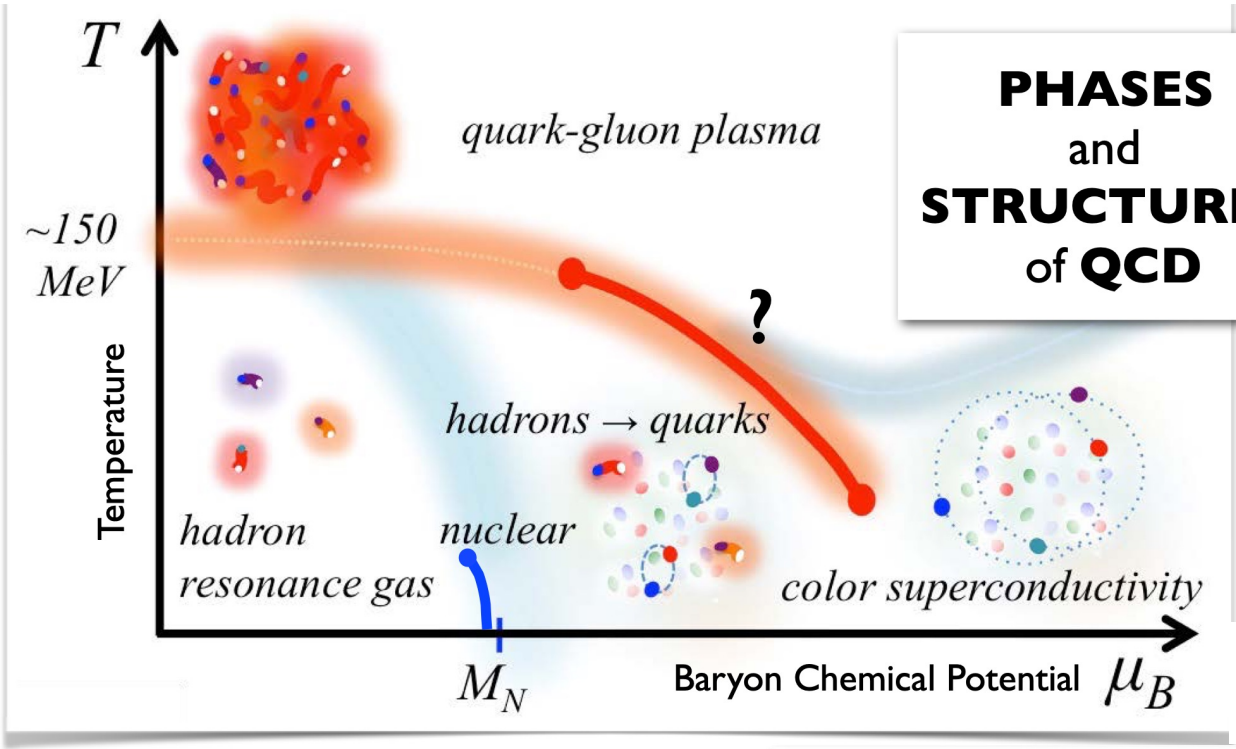

PHASES
and
STRUCTURES
of **QCD**

from:
G. Baym,
T. Hatsuda,
et al.

Rept. Prog. Phys.
81 (2018) 056902

Wolfram Weise
Technische Universität München
PHYSIK
DEPARTMENT

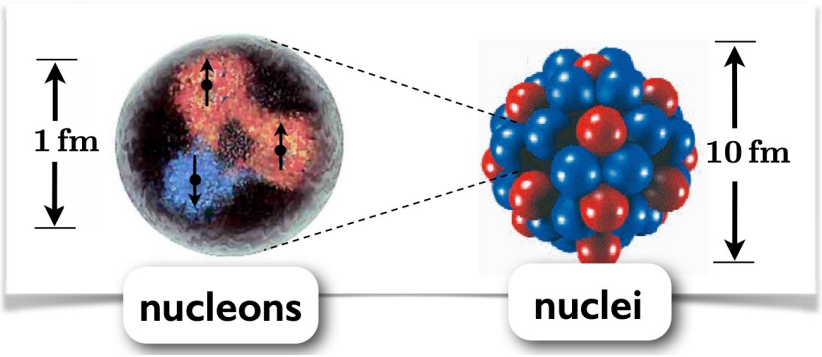

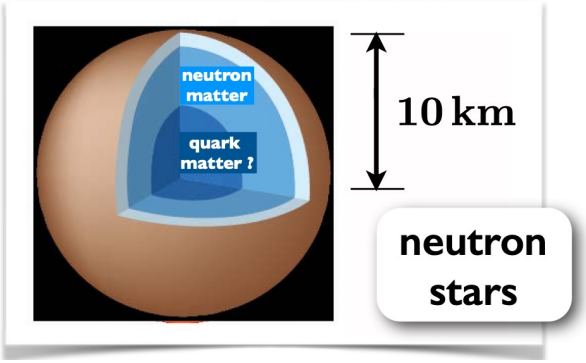

Part I: Hot baryonic matter (HI collisions)

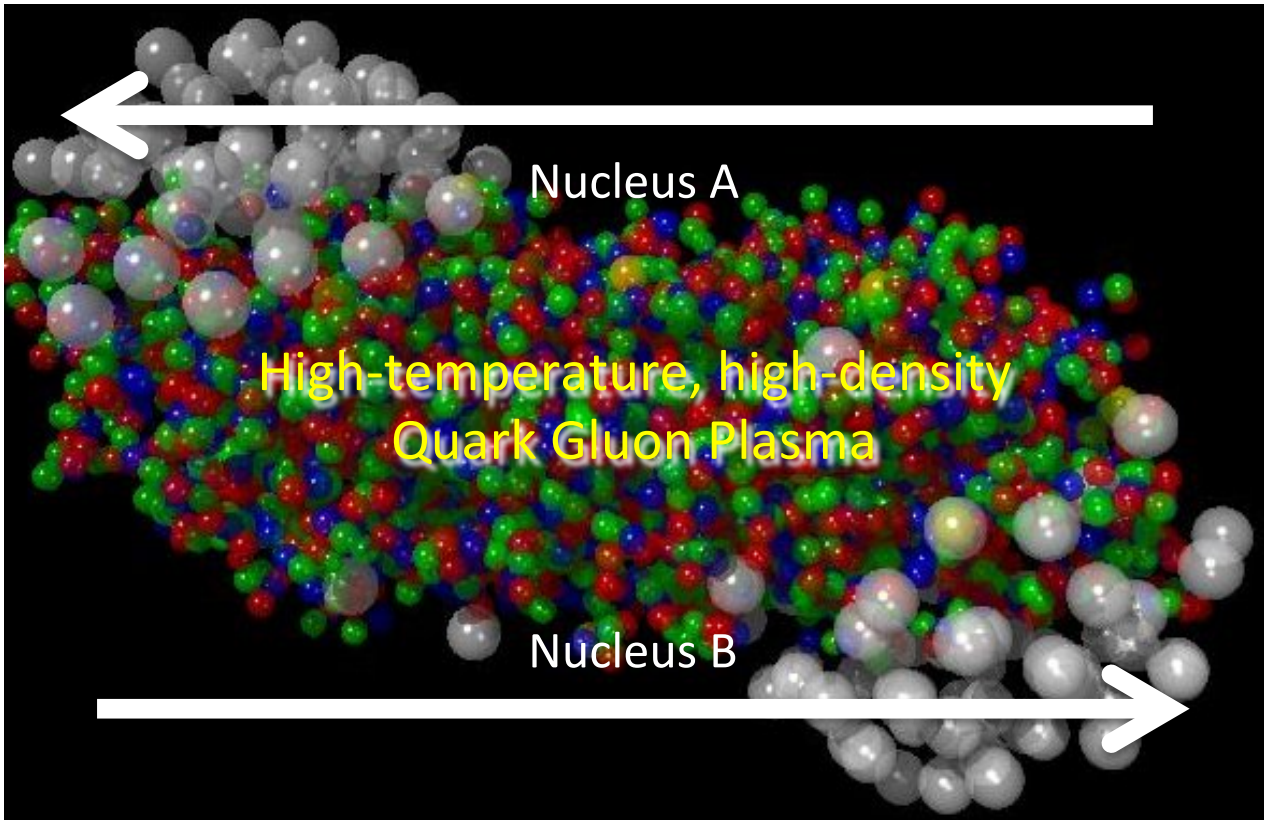

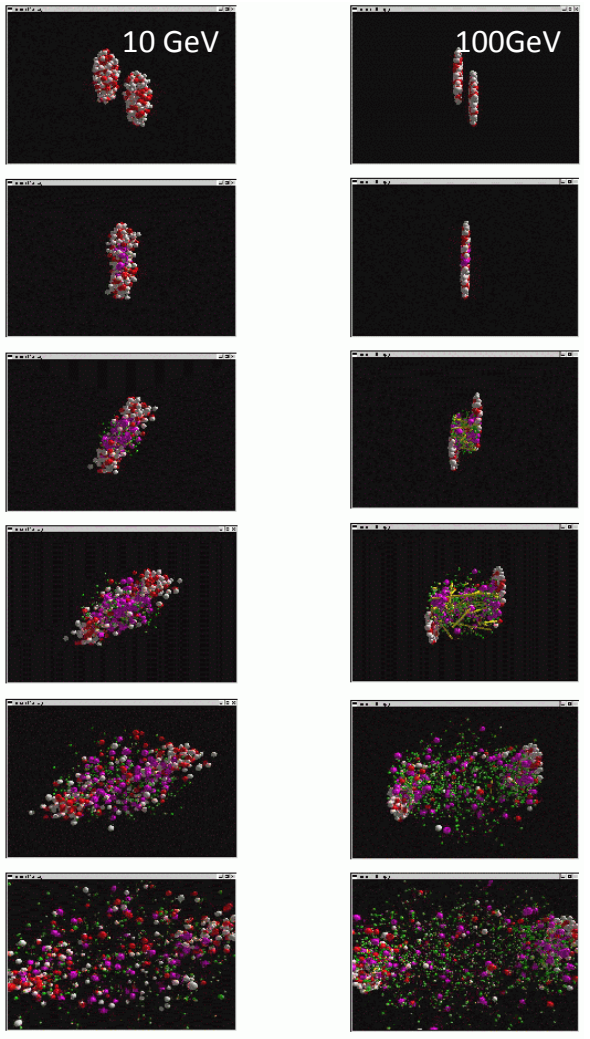

ShinIchi Esumi, Univ. of Tsukuba, TCHoU

“Standard Model” of HI Collisions

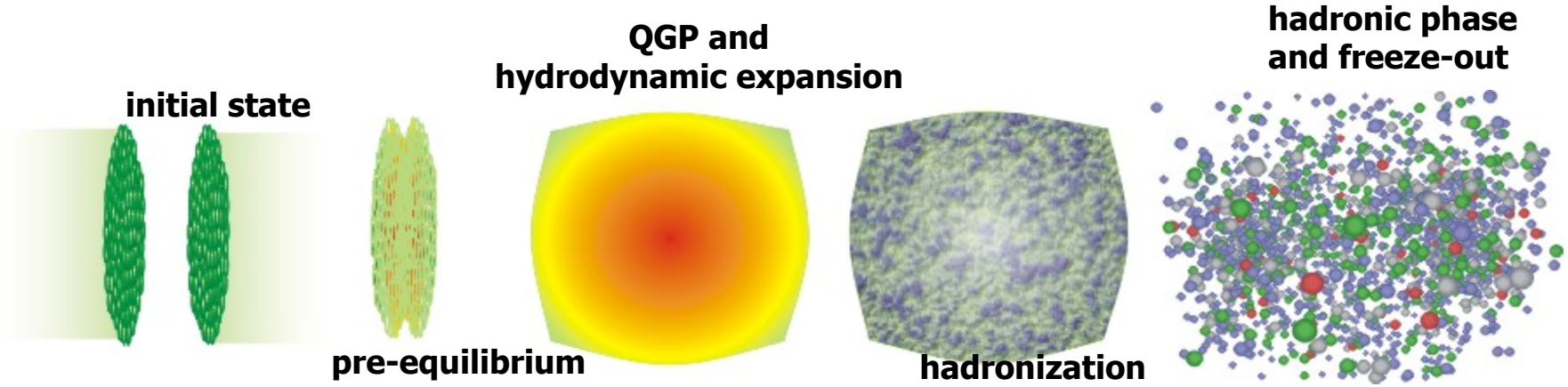

CGC “Glasma” Hydrodynamics Hadronic gas

fast moving nuclei

nuclei collide

expanding & cooling QGP

hadrons re-formed

observed in experiments

High-energy heavy-ion accelerators :
AGS/RHIC at BNL
SPS/LHC at CERN
From few GeV to few TeV

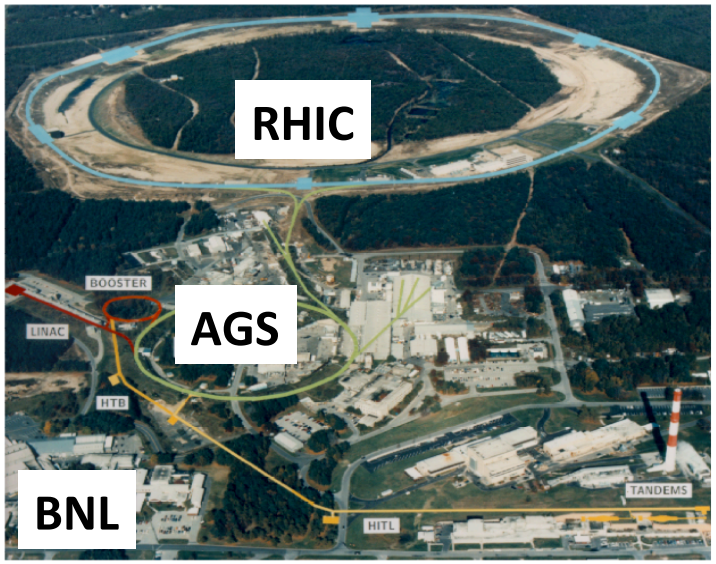

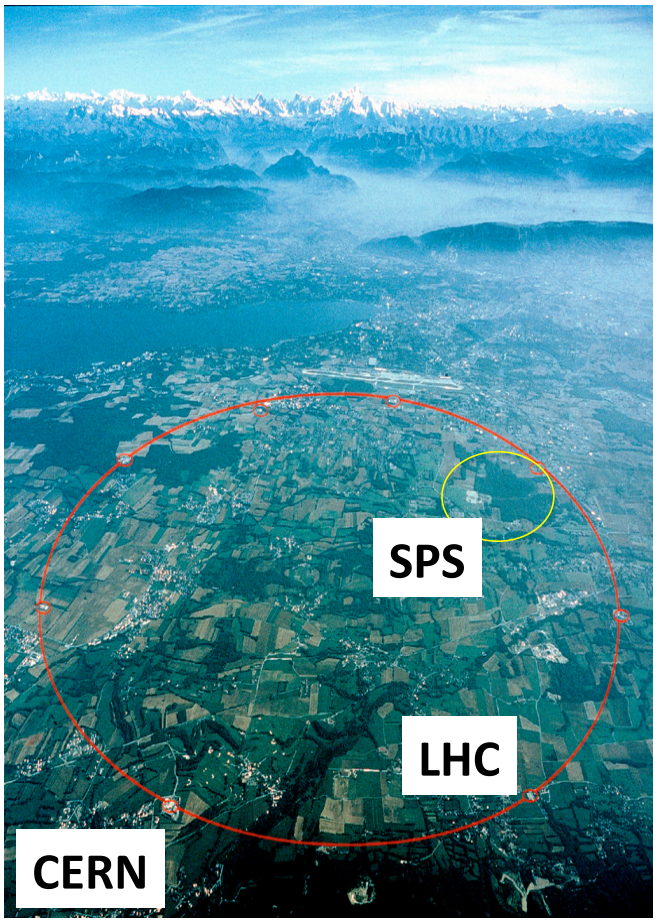

Experiments at RHIC and LHC

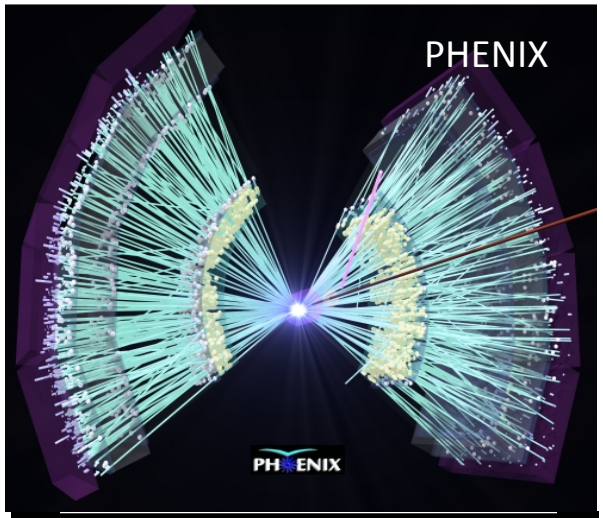

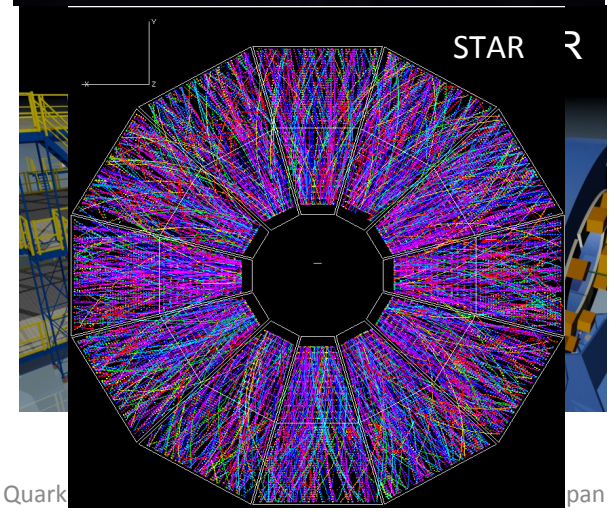

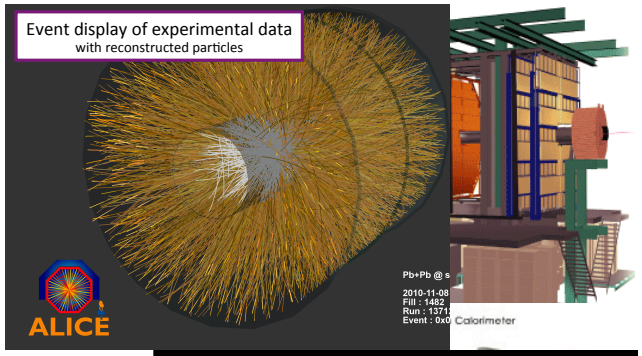

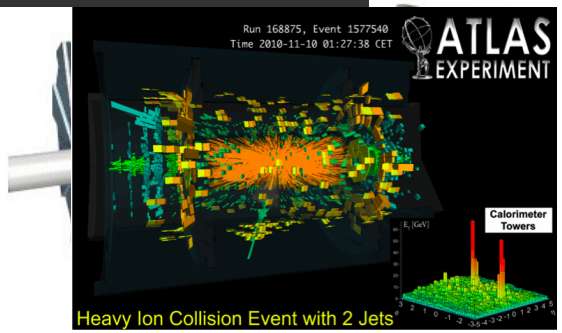

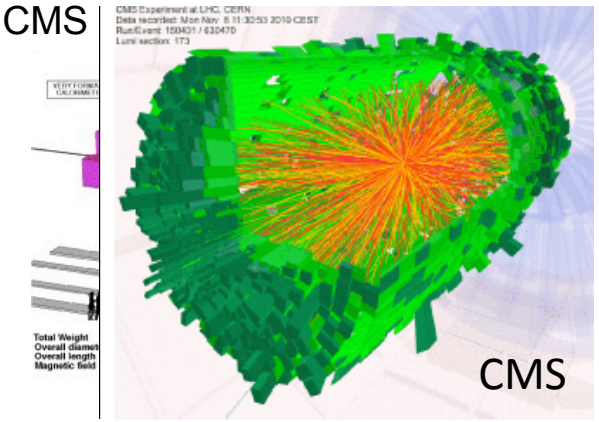

J/ψ suppression and regeneration at LHC

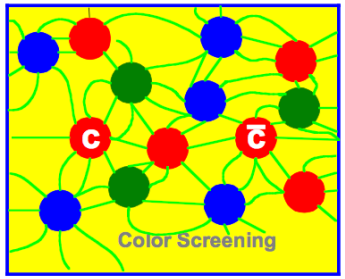

arXiv:1805.04383

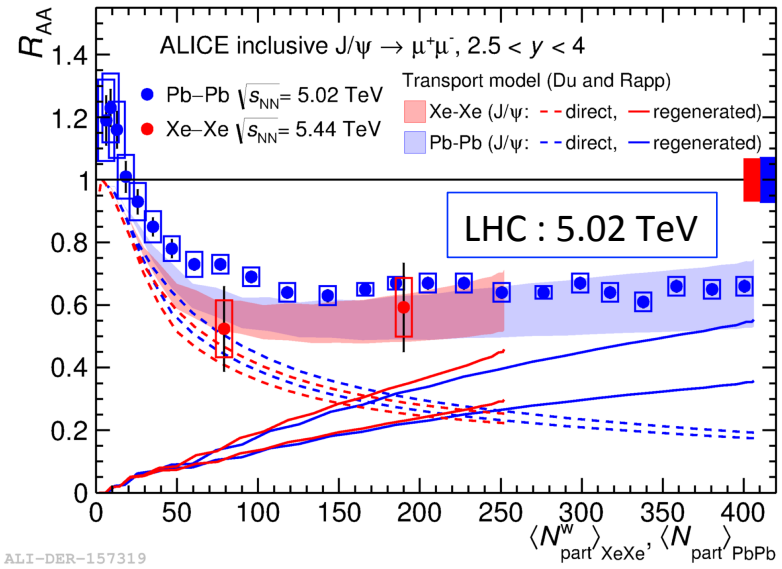

----- Suppression of initial J/ψ

——— Regenerated J/ψ

consistent with charm coalescence scenario
confirmed by J/ψ and charm flow (v_2)

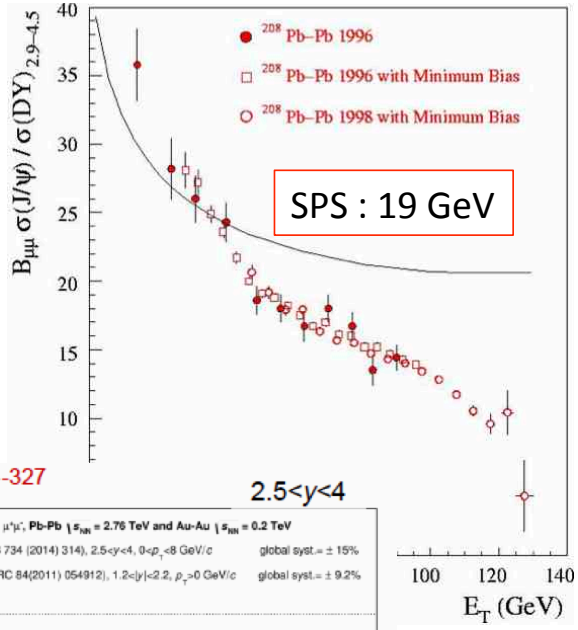

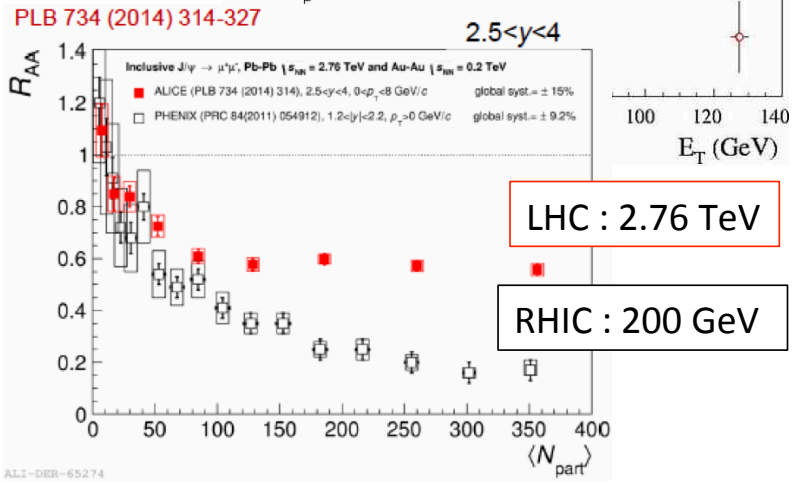

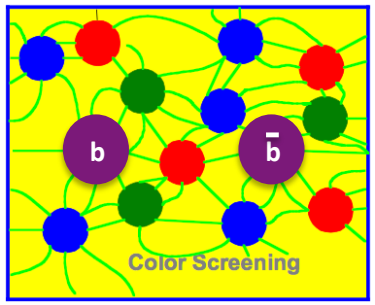

Υ (Upsilon) suppression at LHC

--- more likely from color screening (like J/ψ at SPS/RHIC) ---

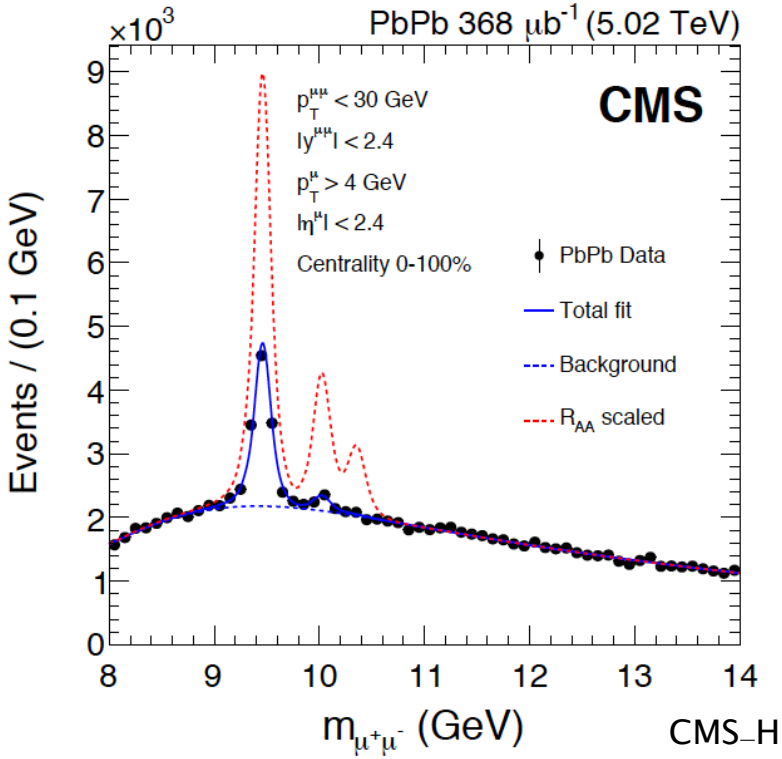

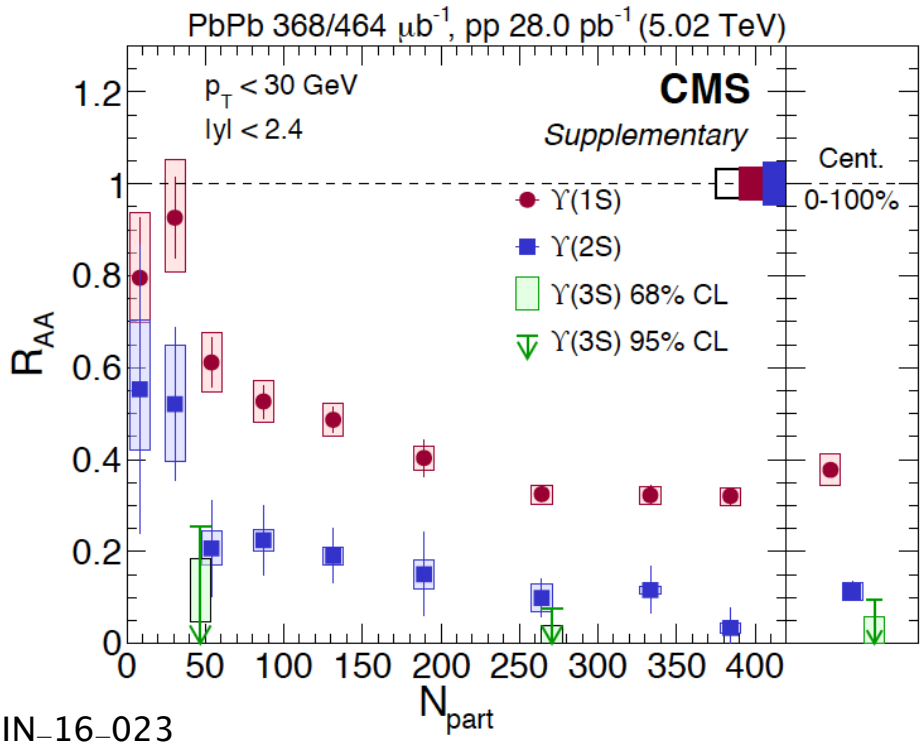

CMS_HIN_16_023

Jet quenching (high p_T suppression)

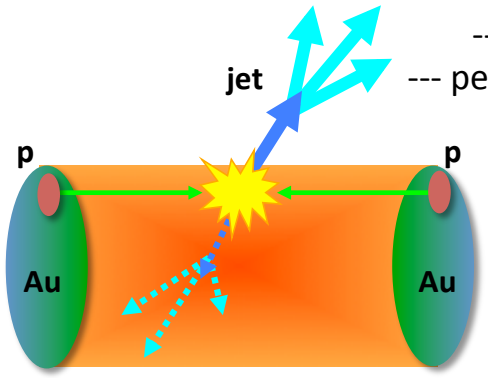

--- partonic energy-loss ---
--- penetration of direct photon ---

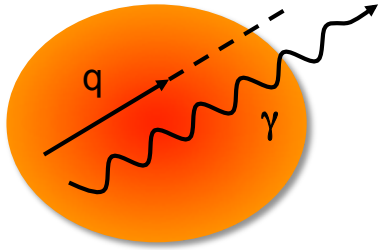

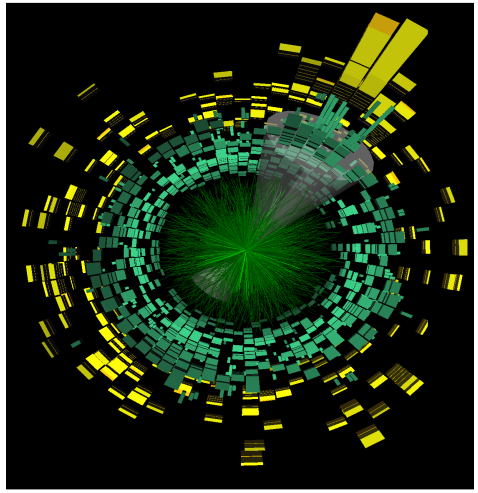

Figure 2.12: A single LHC heavy-ion collision with one high energy jet (upper right) and no apparent partner jet—because it has been quenched by the QGP produced in the collision.

PRL 91 (2003) 072304

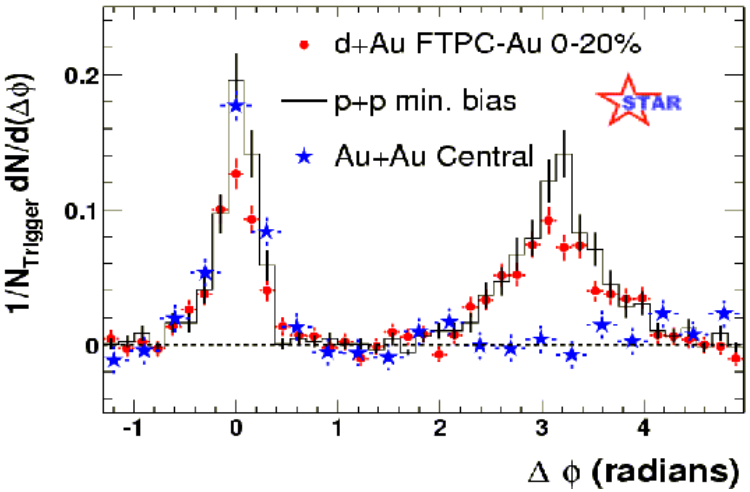

PRL109 (2012) 152302, PRC 87 (2013) 034911

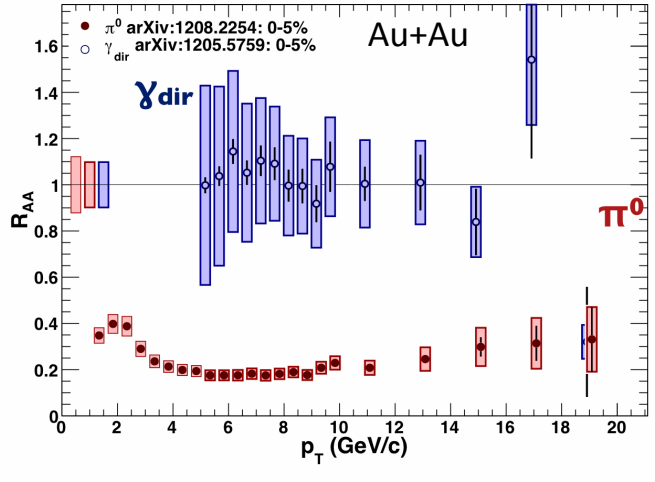

A huge surprise at RHIC was the discovery that QGP is a liquid, a result then confirmed at the LHC. And not just any liquid: it flows with the lowest specific viscosity (characterized in terms of the ratio of shear viscosity to entropy density η/s) of any liquid known, for example, more than ten times smaller than that of water. Over the past five years nuclear physicists have begun to quantify just how perfect the QGP liquid is by virtue of enormous progress on two primary fronts.

the η/s of QGP is very close to a fundamental quantum limiting value deduced for the extreme hypothetical case when the quarks and gluons have infinitely strong interactions

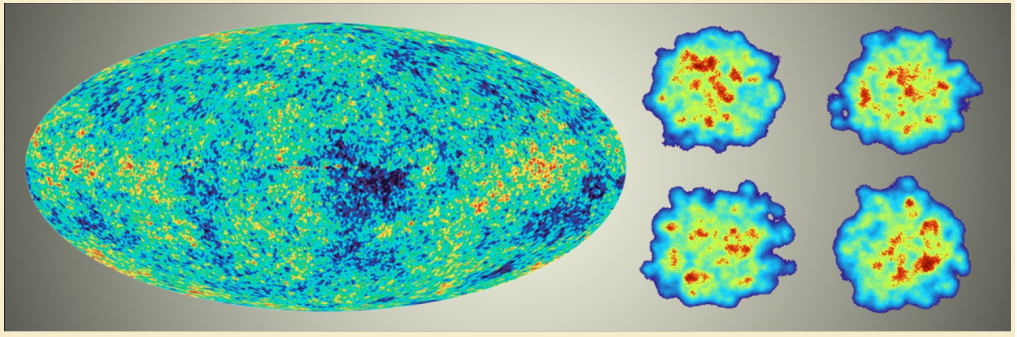

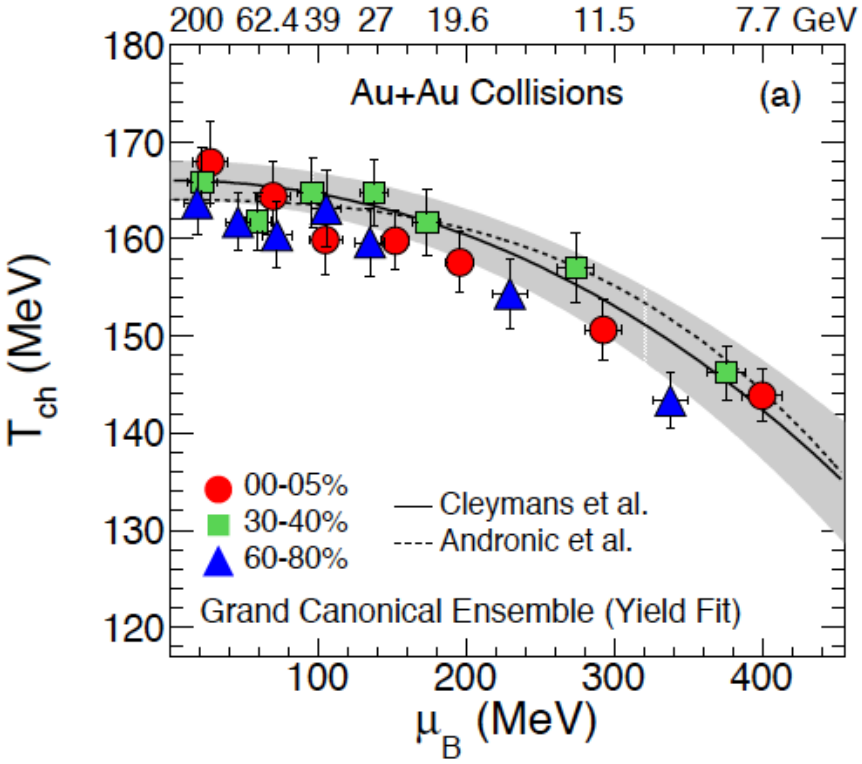

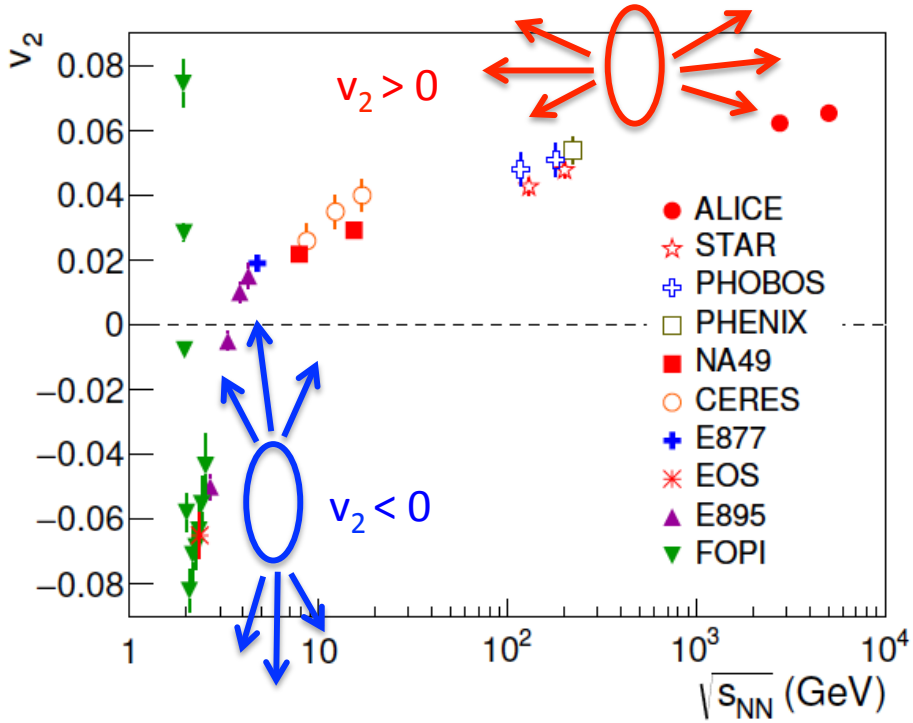

Phys. Rev. Lett. 118 (2017) 212301

Baryon density increases with decreasing beam energy.

v_2 evolution with beam energy and quark coalescence

Flow in small systems

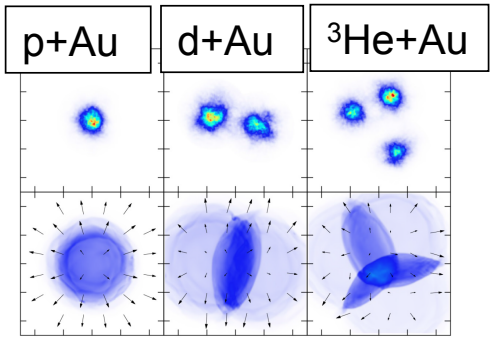

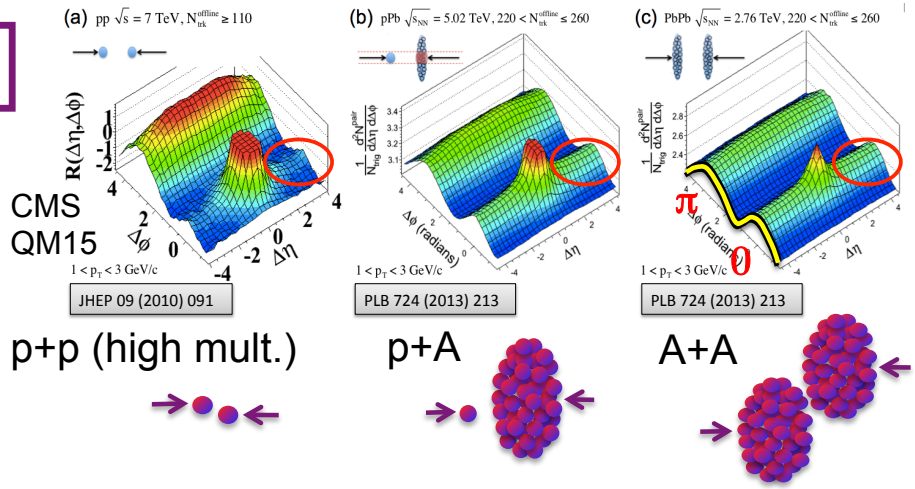

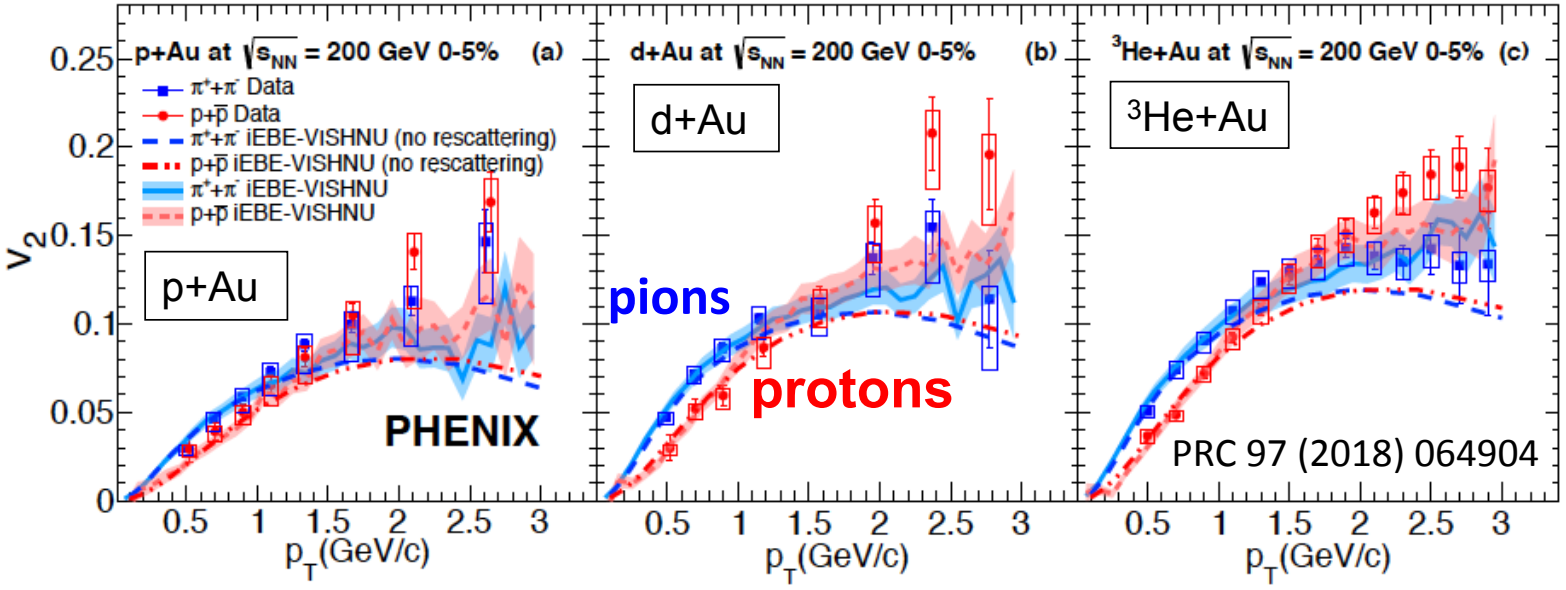

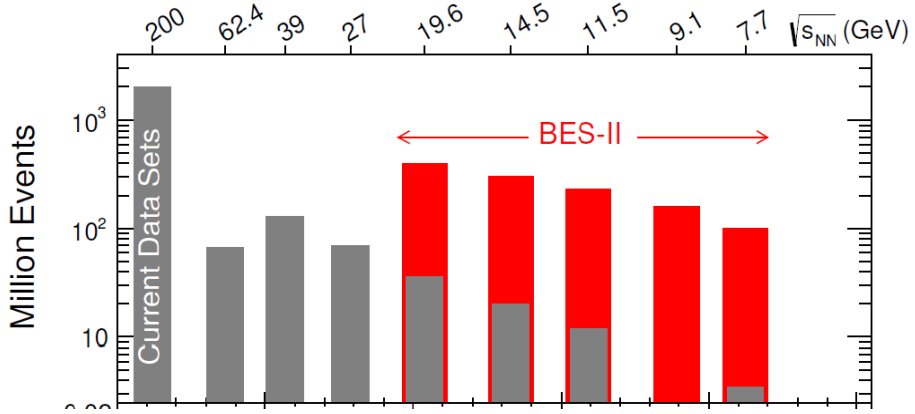

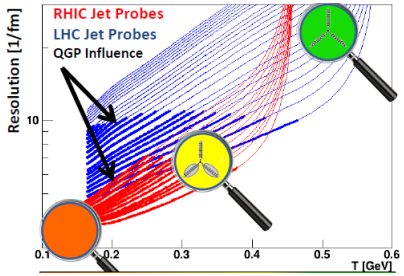

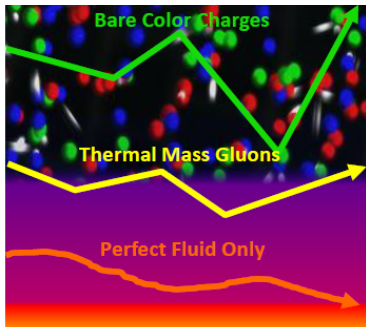

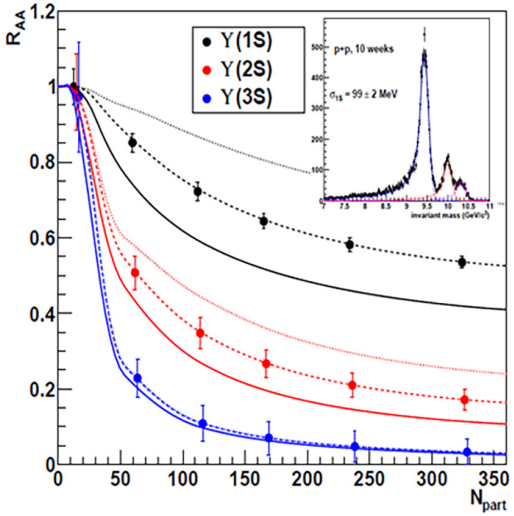

Figure 2.11: *The projected sPHENIX mass separation of the three upsilon states (in the inset) and the projected accuracy of measuring their nuclear suppression in collisions with varying impact parameters. Three sets of theory curves show the melting dependence on the degree of fluid perfection.*

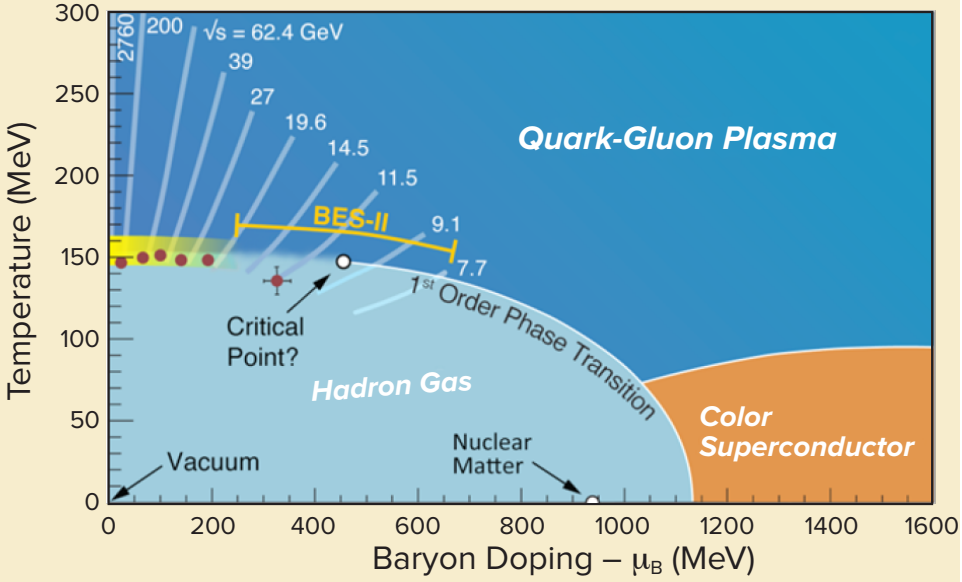

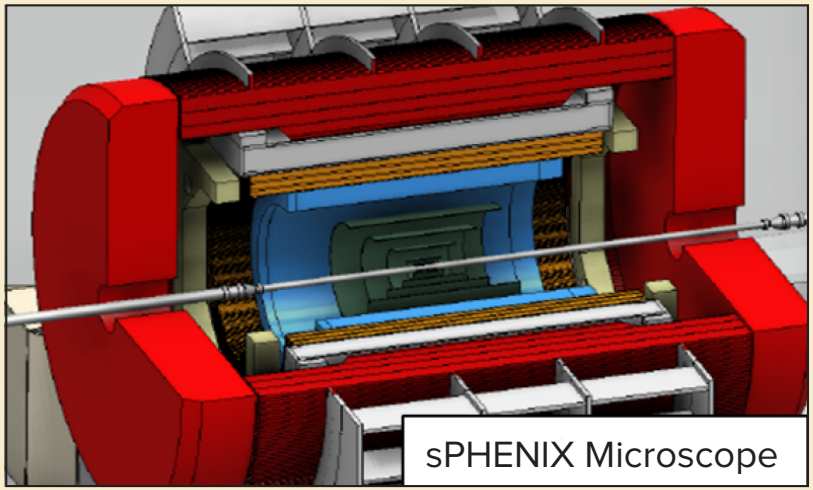

Heavy-ion collisions and neutron star merger

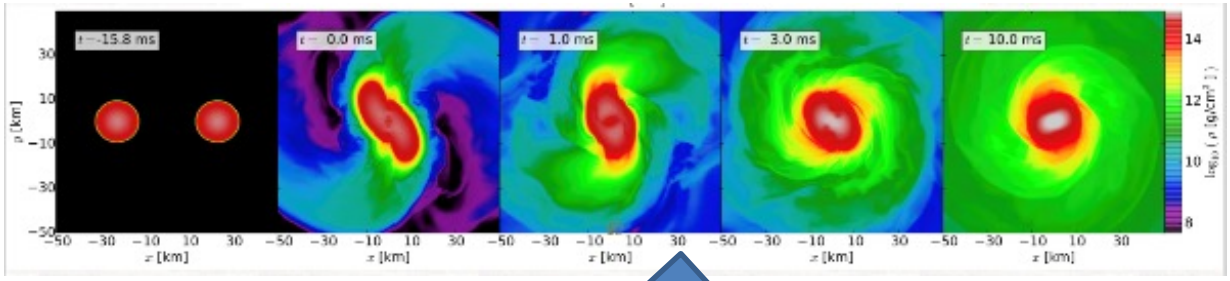

M. Hanauske, J. Steinheimer (priv. com.)
L. Rezzolla et al. arXiv:1807.03684

Gravitantional wave signal can probe the dense EOS during “ring down“ if frequencies in kHZ range are detected.

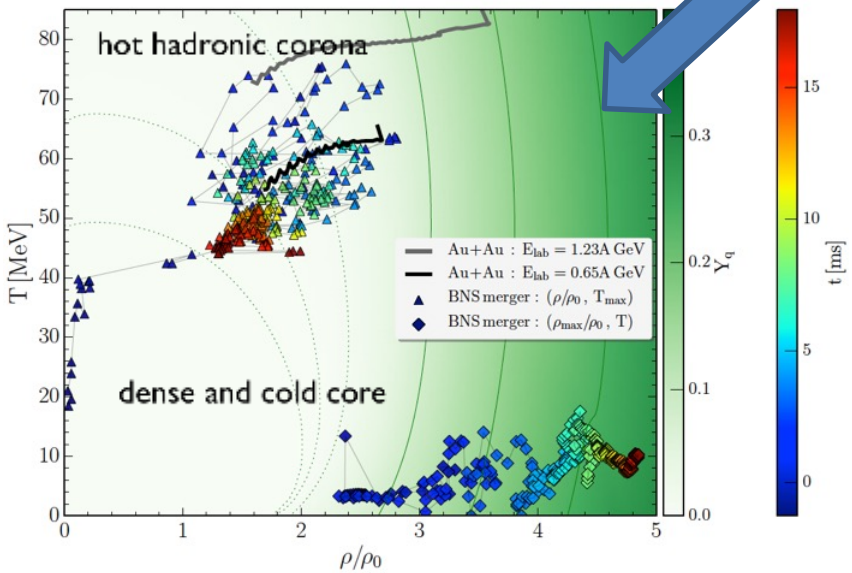

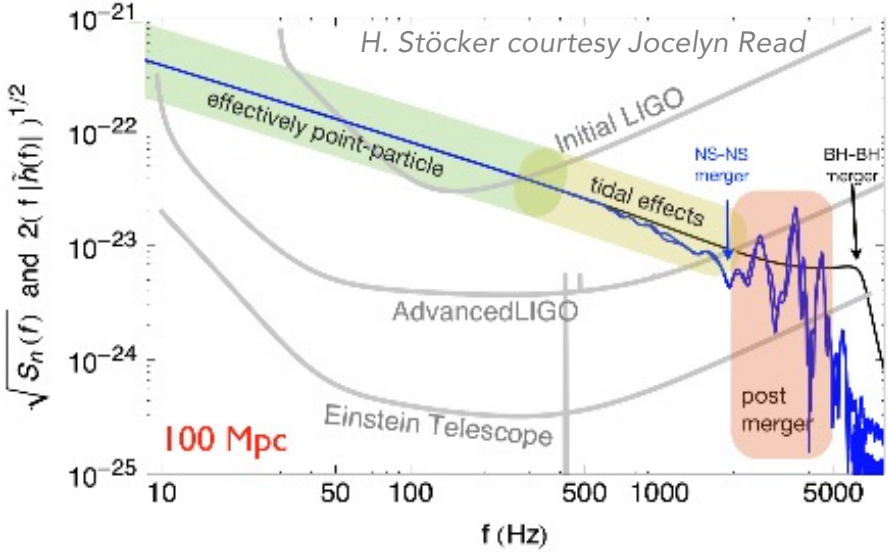

Current facilities for high μ_B physics

NA61 – SPS

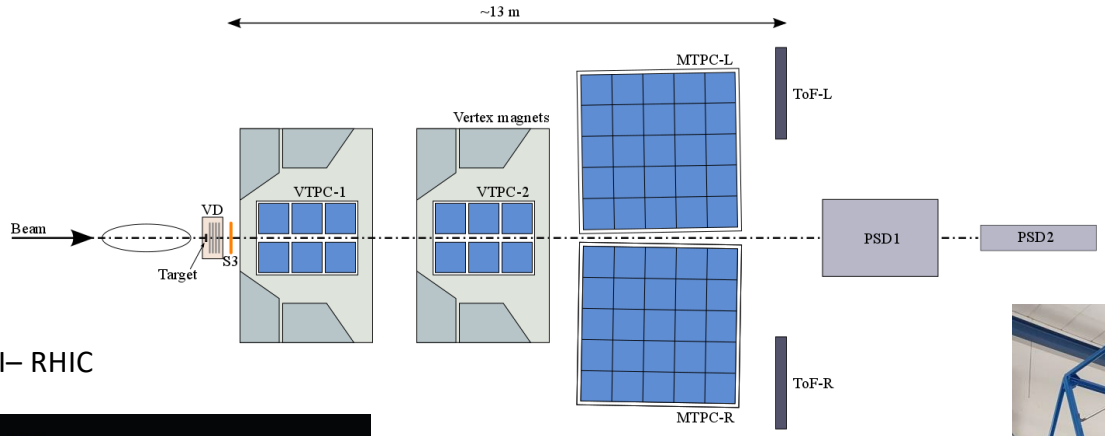

STAR-*BES*II– RHIC

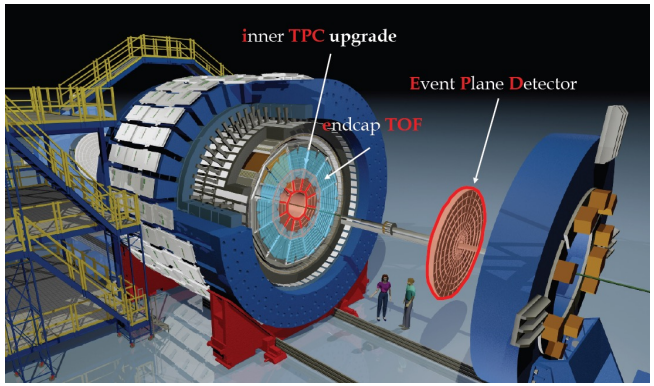

HADES – FAIR

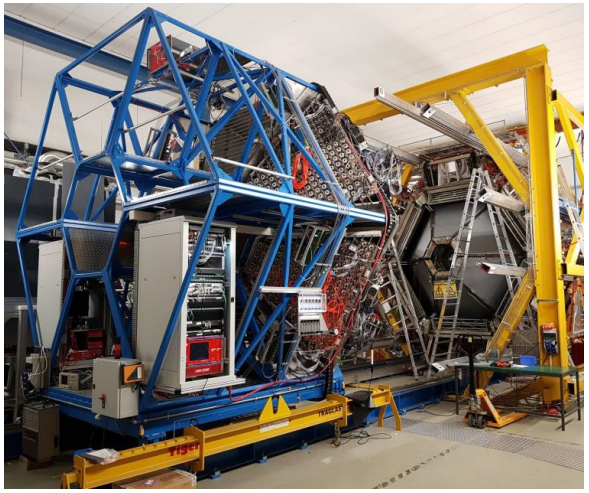

Future facilities for high μ_B physics

NA60⁺ – SPS

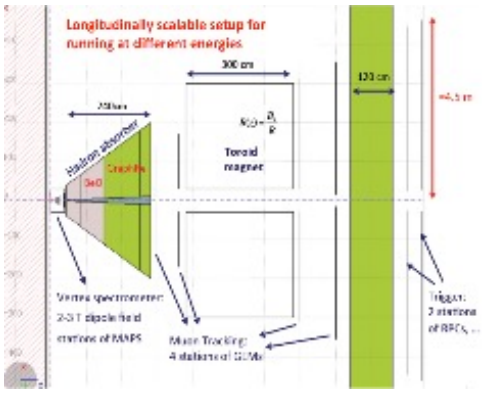

MPD – NICA

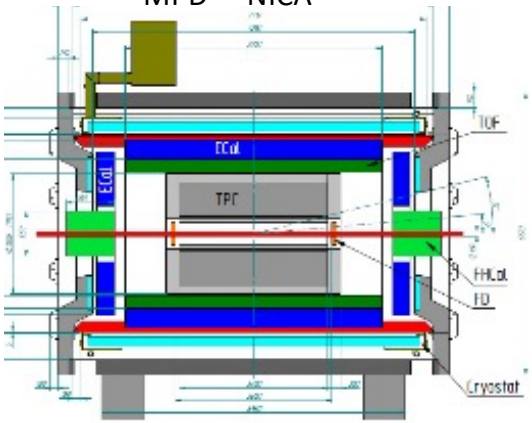

CBM– FAIR

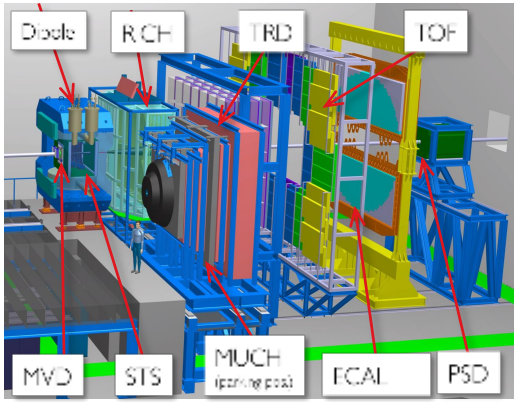

DHS – *J*PARC-HI

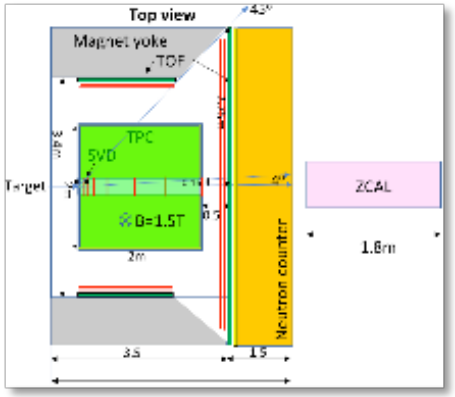

BM@N – NICA

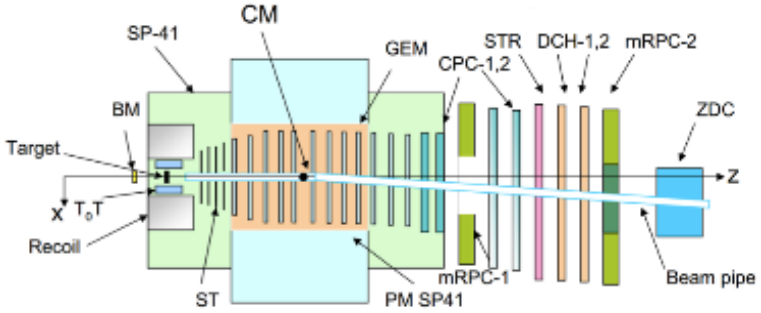

CEE– HIAF

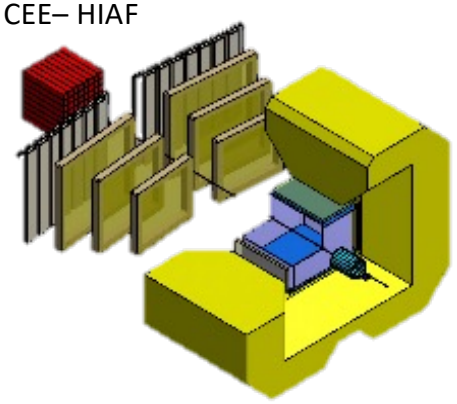

Yet another potential phase of QCD matter

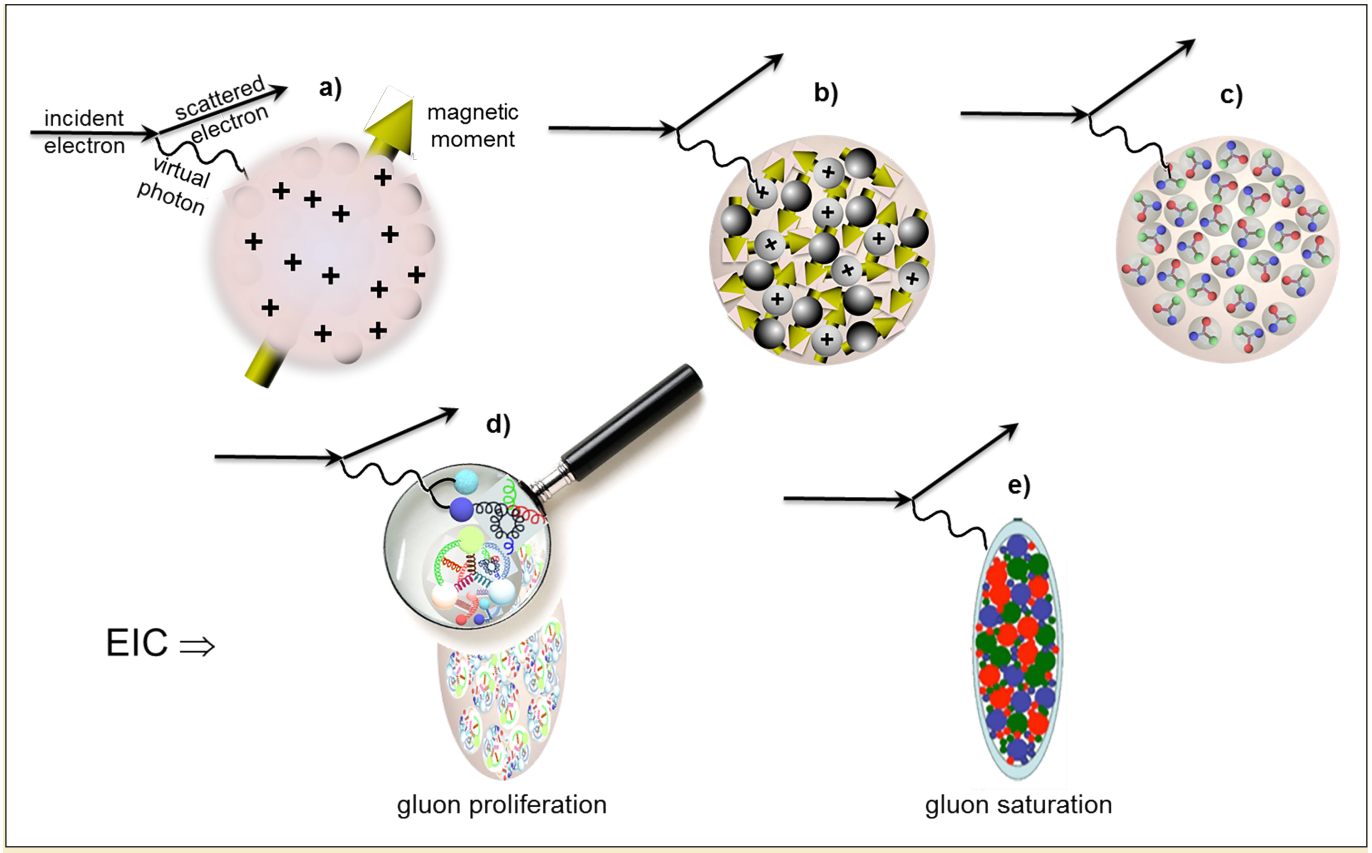

QCD Matter at Extreme Gluon Density

What happens to the gluon density in nuclei at high energy? Does it saturate, giving rise to a gluonic matter component of universal properties in all nuclei, even the proton? How does the nuclear environment affect quark and gluon distributions and interactions inside nuclei? Do the abundant low-momentum gluons remain confined within nucleons inside nuclei?

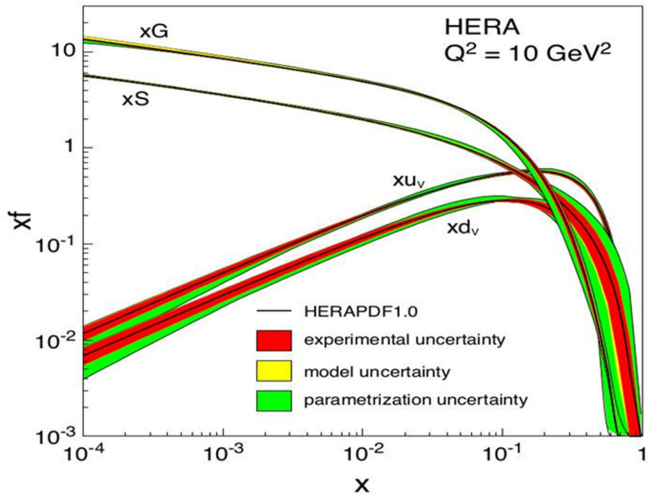

FIGURE 2.8 A global fit to parton distribution functions of the proton based on deep inelastic scattering data obtained at the Hadron-Electron Ring Accelerator (HERA). Distribution of gluons, G, sea quarks, S, and valence up and down quarks, u_v and d_v, are shown as a function of Bjorken *x*. SOURCE: Adapted from H. Abramowicz et al., 2015, Combination of measurements of inclusive deep inelastic $e^{\pm}p$ scattering cross sections and QCD analysis of HERA data, *Eur. Phys. J.* C75:580.

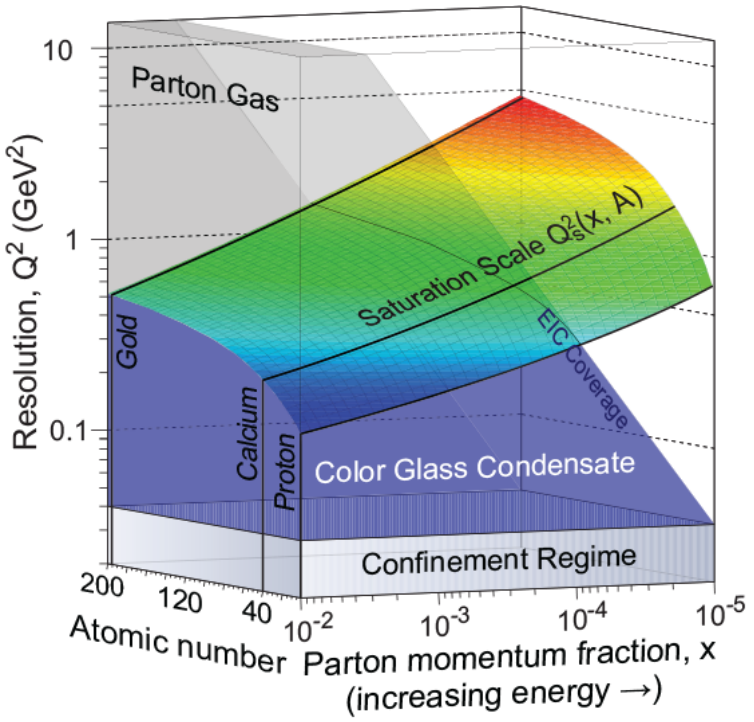

Figure 2.18: *The schematic QCD landscape in probe resolving power (increasing upward) vs. energy (increasing toward the right), as a function of the atomic number of the nucleus probed. Electron collisions with heavy nuclei at the EIC will map the predicted saturation surface (colored surface) with the CGC region below that surface. Spatial distributions extracted from exclusive reactions (see text) will help demarcate the CGC region from the confinement regime.*

Machine to study this Physics: Electron – heavy ion collider

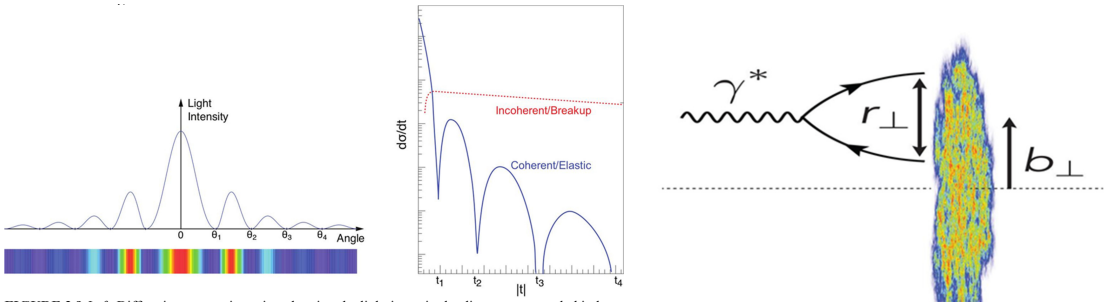

FIGURE 2.9 *Left*: Diffraction pattern in optics, showing the light intensity landing on a screen behind a circular obstacle. *Right*: The expected differential cross section for coherent and incoherent diffractive production of J/ψ particles on nuclei. The variable *t* is related to the momentum carried by the virtual photon, which is a measure of the scattering angle. The incoherent/breakup curve is explained in the text. SOURCE: *Reaching for the Horizon*, 2015 DOE/NSF Long Range Plan for U.S. Nuclear Science.

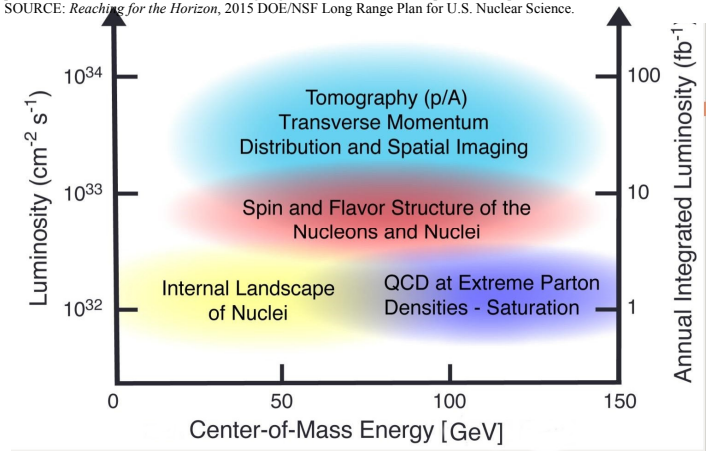

FIGURE 2.4 The energy-luminosity landscape that encapsulates the physics program of an Electron-Ion Collider. The horizontal axis shows the center-of-mass energy of the collider when operated in electron-proton mode. The two vertical axes show the instantaneous and annual integrated (electron-nucleon) luminosity; the latter is in units of inverse femtobarns, and assumes a running time of 10^7 seconds per year. SOURCE: Presentation of EIC Science by A. Deshpande on behalf of the EIC Users Group

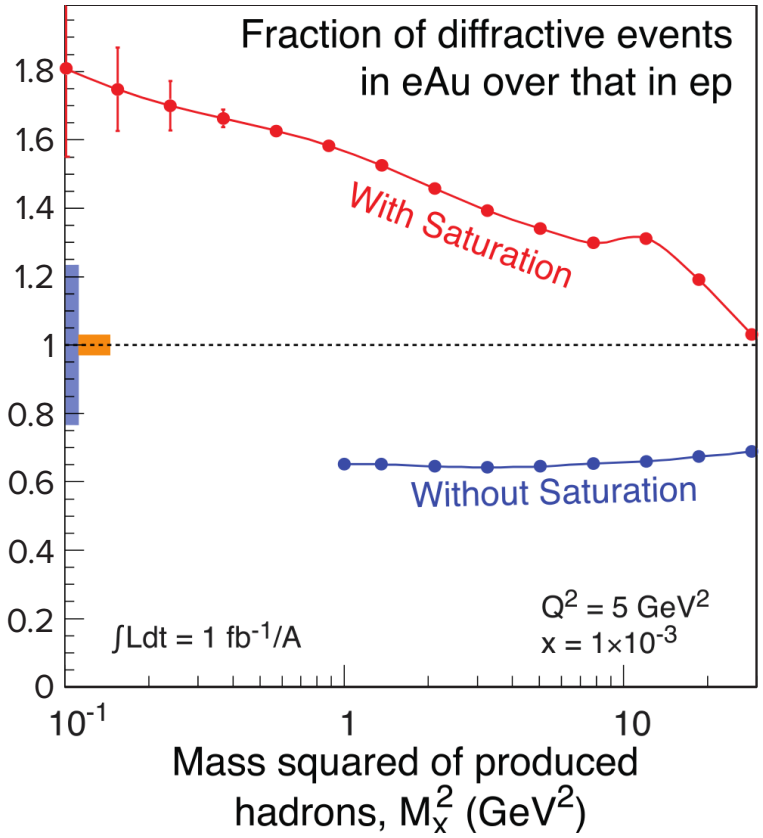

Figure 2.19: *The ratio of diffractive over total cross section for DIS on a gold nucleus normalized to DIS on a proton, for different values of the mass-squared of hadrons produced in the collisions, predicted with (red curve) and without (blue curve) gluon saturation. The projected experimental uncertainties are smaller than the plotted points while the range of each model's prediction (shaded bands on the left side) is smaller than the difference caused by saturation.*

Applications of Nuclear Physics

- Radiation Detectors -> Medicine, materials, climate, security
- Accelerators; gamma ray and synchrotron sources, FELS
- Radioactive elements for medicine and industry
- Nuclear Power
- Isotope dating, Forensics
- Radiation protection
- Defense

Tools of fundamental research

We build particle detectors big…

…and small:

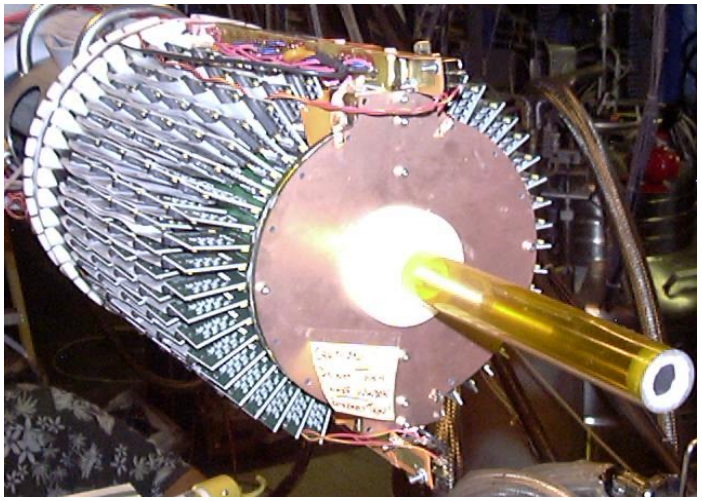

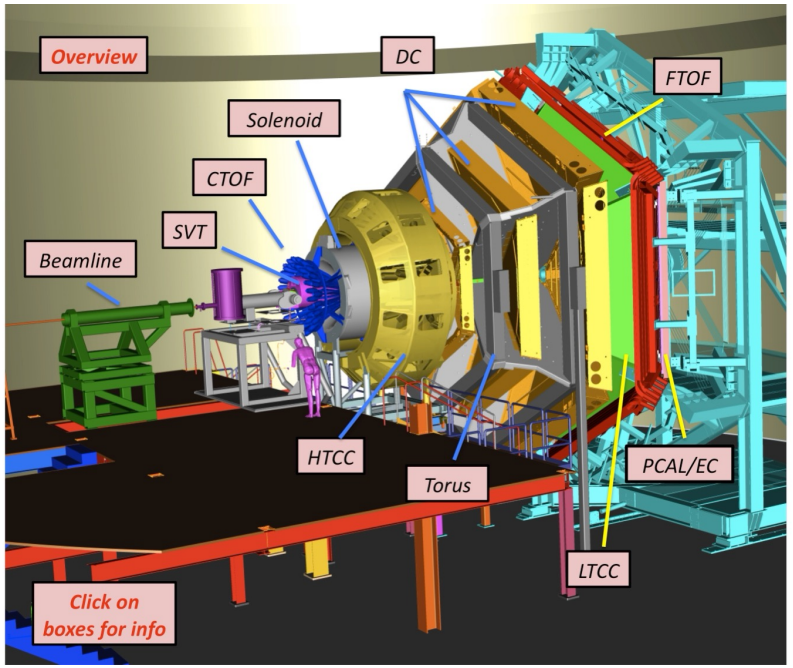

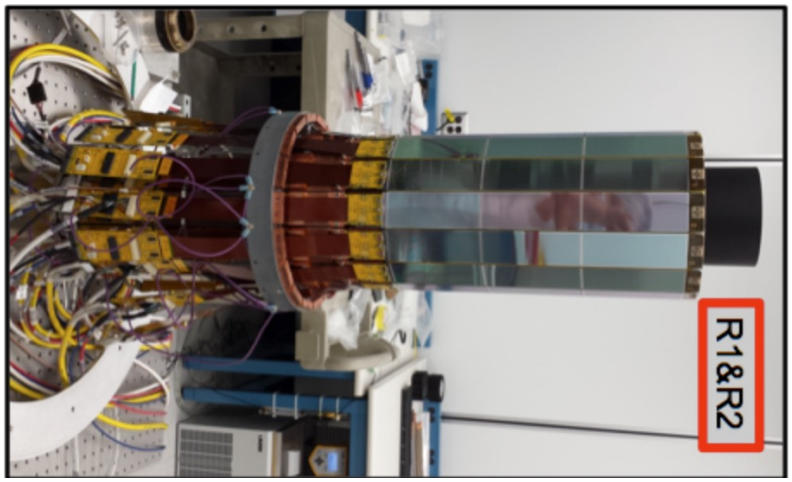

…that can be used for a wide variety of applications:

Ion Beam Analysis of Consumer Products

- **Perfluorinated compounds (PFCs)**: fluorine-containing chemicals with unique properties to make materials stain- and stick-resistant. Some PFCs are incredibly resistant to breakdown and are turning up in unexpected places.
- PFOA is a likely human carcinogen.

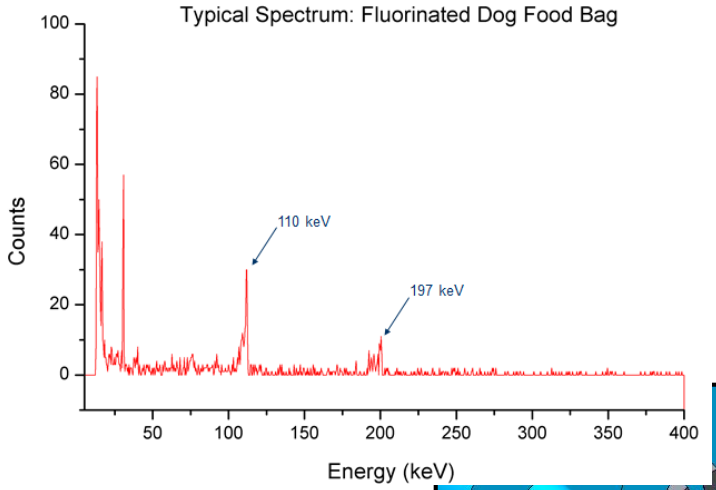

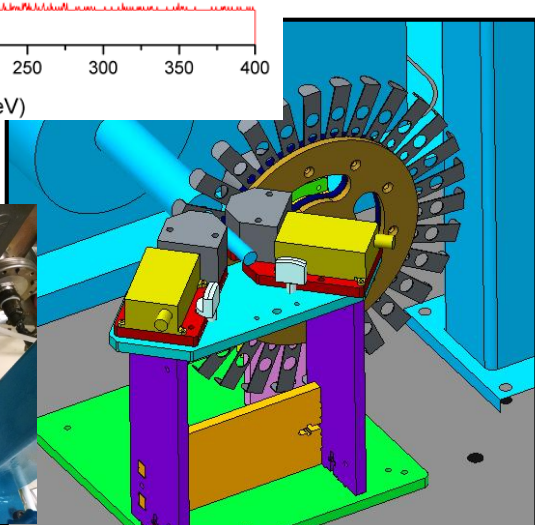

Look at PhysicsToday Article
“Medical Imaging with Antimatter”

Large Field of View Positron Emission Mammography Imaging Devices

graphy (PEM)
nsitivity, high
PET for
ion with Duke
gton, PI), we
large field of
e device is
O/LYSO crystal
oact position
e-clinical trials
; 4 mm were
dvanced
hms developed
rials at Duke
) showed that
n be imaged.
is underway to
ast cancer

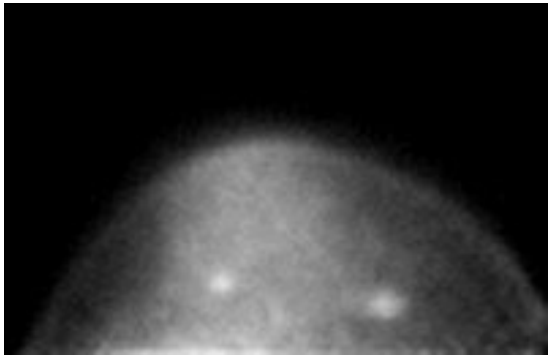

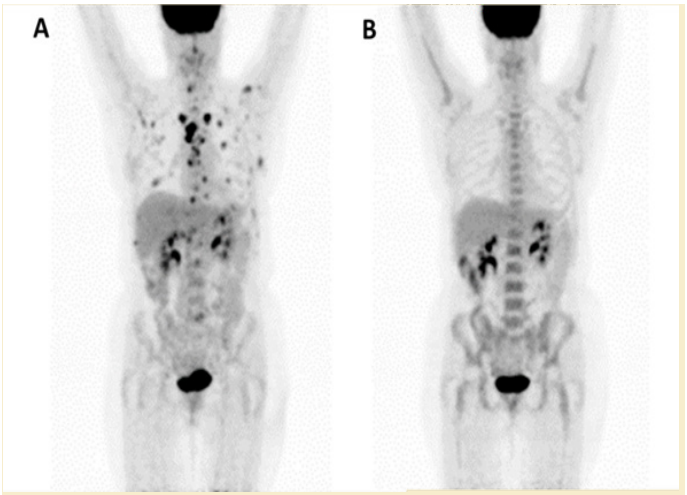

[^{18}F] fluorodeoxyglucose scan of a woman diagnosed with T cell lymphoma. (A) At diagnosis, which shows uptake in extensive disease sites along with normal signal in the brain and bladder. (B) Following four months of chemotherapy, which shows the dramatic decrease in signal in the cancer sites, indicating that this patient is responding well to therapy. Image credit: J. McConathy.

Plant Biology Imaging

$^{11}CO_2$ (half life = 20 min.)

Translocation of sugars in corn – indicator of environmental conditions

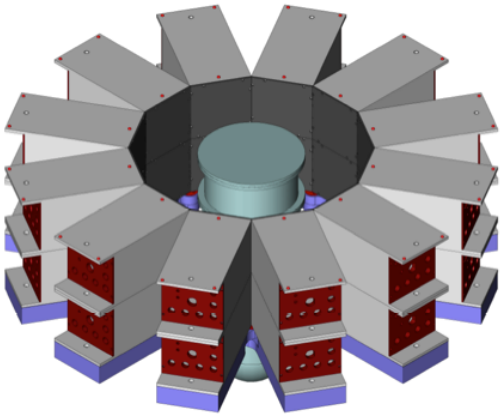

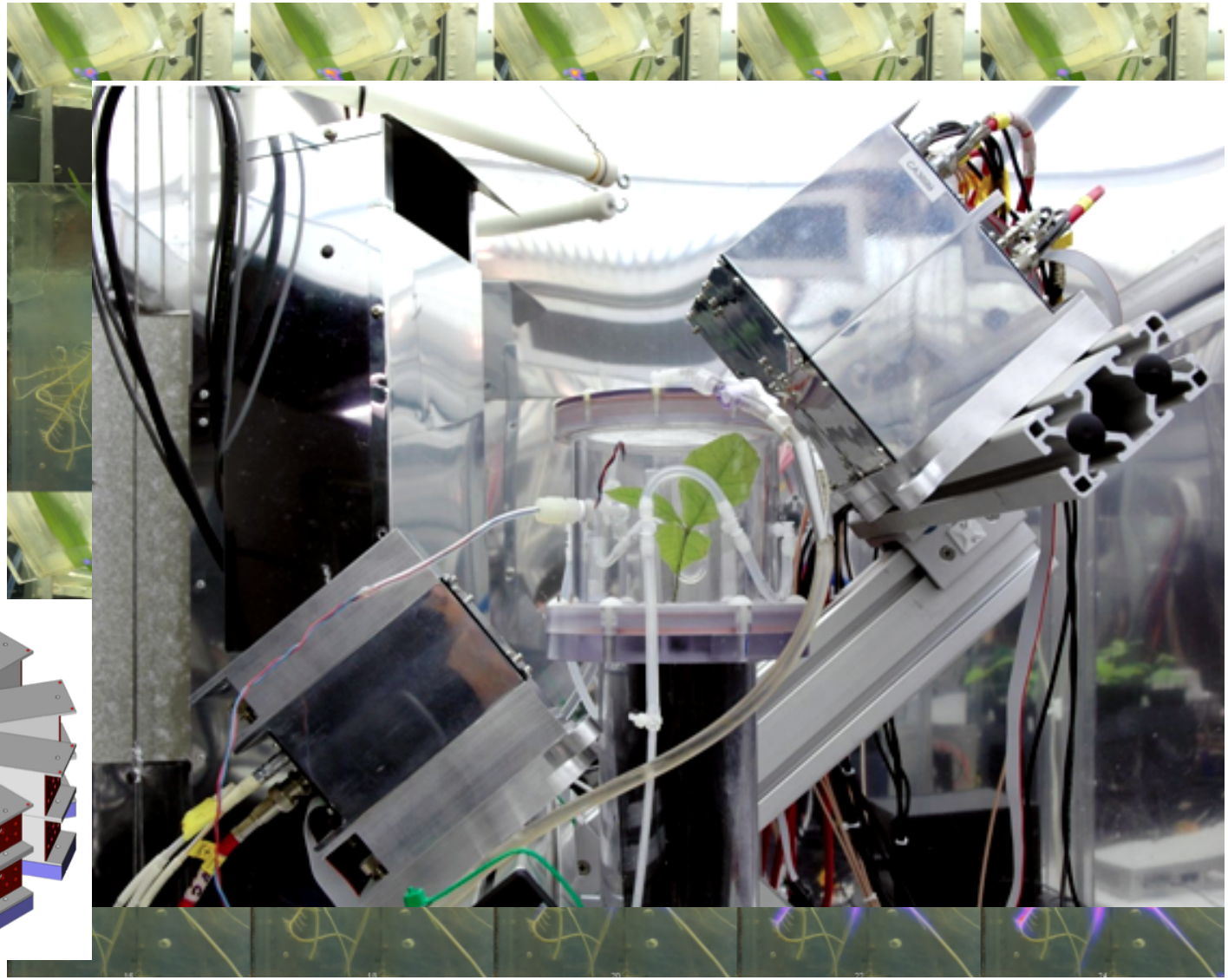

Awake Animal SPECT Project

The Jefferson Lab Detector and Imaging Group in collaboration with Oak Ridge National Laboratory (Dr. Justin Baba), Johns Hopkins University (Dr. Martin Pomper) and the University of Sydney (Dr. Steve Meikle) is developing an imaging methodology that utilizes SPECT and X-ray CT for small animal research. The primary challenging task of this project is to develop a SPECT imaging system to allow molecular imaging of unrestrained and un-anesthetized mice. Present methods of performing SPECT imaging with mice require the animals to be anesthetized or physically restrained during image acquisition. Both methods of restraint have the potential to interfere with the physiological and neurological processes being investigated. In the initial focus of the project, tracking of the orientation and location of the mouse's head during SPECT imaging is accomplished through a pair of CMOS optical cameras that image IR retro-reflectors attached to the mouse's head. The gamma-ray projection data is reconstructed into a fixed small animal reference frame based on the time-varying animal orientation data. The goal is to develop instrumentation to acquire high-resolution volumetric SPECT images of the head region of an unrestrained, un-anesthetized mouse and to register these image volumes with microCT data sets of the same mouse acquired before or after the SPECT scan. The animal will be anesthetized during the microCT scan. Jefferson Lab is coordinating the entire effort and is developing high spatial resolution gamma cameras 10 cm x 20 cm in size for the SPECT system. The system is installed in the animal research facility at Johns Hopkins University where it is being tested with awake mice.

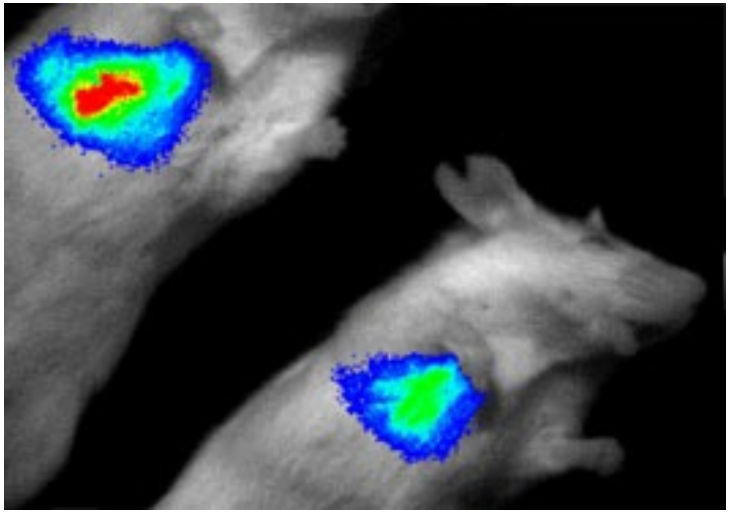

…and oil exploration, fluid dynamics, material imaging, climate model testing, nuclear reactor monitoring, radioactive element detection, space radiation mapping, CT, PET, …

…and even **NMRI**!

Looking for dangero

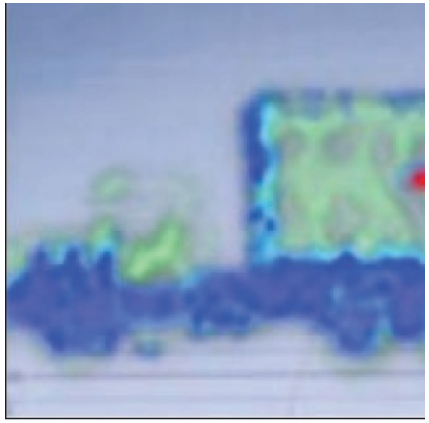

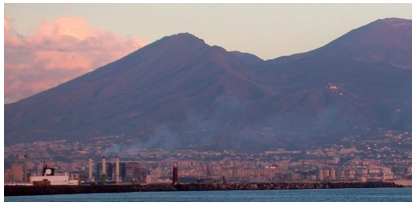

…or monitoring a c
(Vesuvius)…

An international team of scientists has discovered a large hidden cavity within Egypt's Great Pyramid of Giza, and they did it by looking for muons — particles sent to Earth by cosmic rays from space.

The mysterious cavity, described Thursday in the journal Nature, is at least 30 meters long. And though the researchers aren't sure whether it's straight or inclined, whether it's one large space or a series of smaller ones, the discovery has already triggered interest among archaeologists as to the purpose of the void.

"What we are sure about is that this big void is there," said Mehdi Tayoubi, president of the nonprofit Heritage Innovation Preservation Institute in Paris, which led the effort. "But we need to understand [it] better."

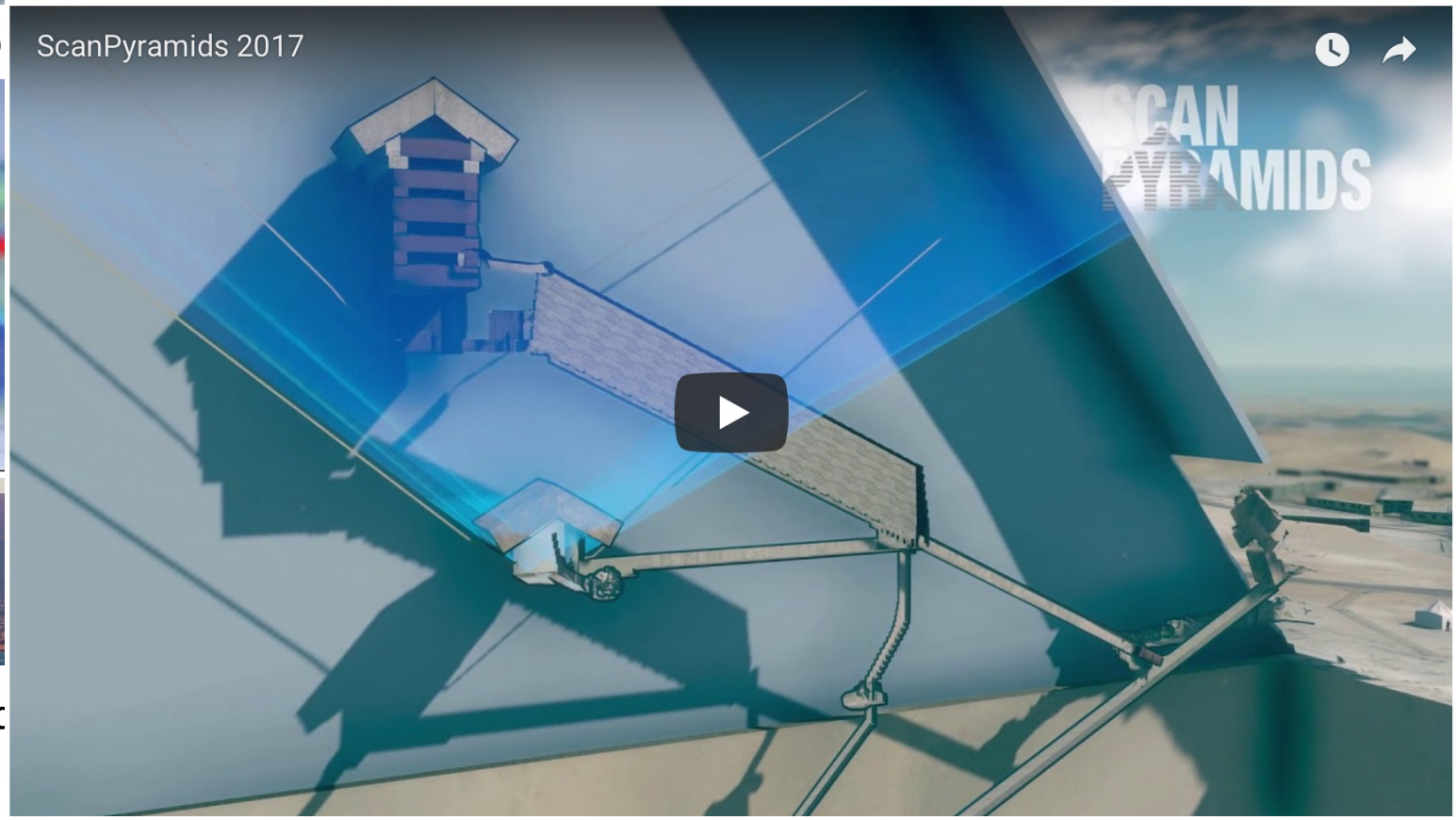

Nuclear Science in Art and Archaeology

luminescence dating, and methods of archeometry.

Figure 1: *A University of Missouri researcher characterizing an ancient Roman artifact (photo credit Nic Brenner, University of Missouri).*

Figure 2: *Figurine found in Mesoamerican burial grounds and currently housed at the University of Notre Dame's Snite Museum of Art. The figurine is mounted on the proton-induced X-ray emission (PIXE) beam line at Notre Dame's 11-MV electrostatic accelerator to obtain quantitative details of the pigment composition; in particular, PIXE reveals the iron and manganese content of the paint.*

Accelerators in Industry and Medicine

Hampton University
Proton Therapy Institute

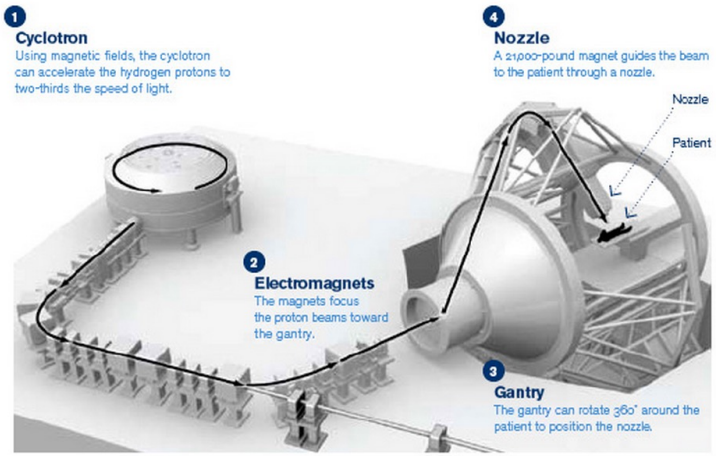

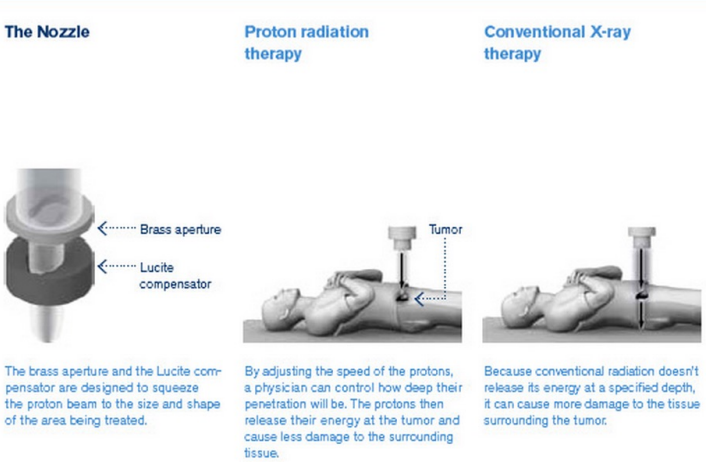

…even more examples

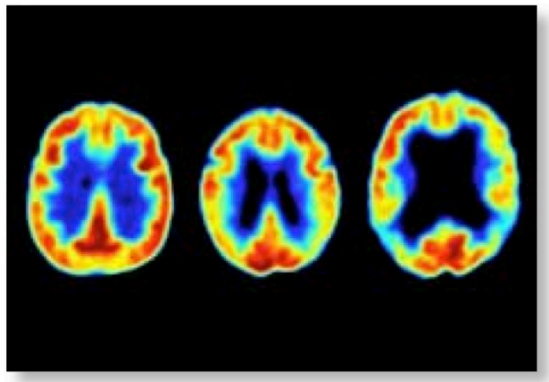

PET scans reveal reduced brain activity in people with Alzheimer's disease (right) and cognitive impairment (center).

Advances in accelerator physics have led to more effective cancer-killing beams.

The Cassini spacecraft gets power from plutonium, a nuclear isotope.

Techniques developed by nuclear physicists eliminate potential pathogens in our food supply.

Developing innovative detectors is crucial to identifying hazardous materials in shipping containers.

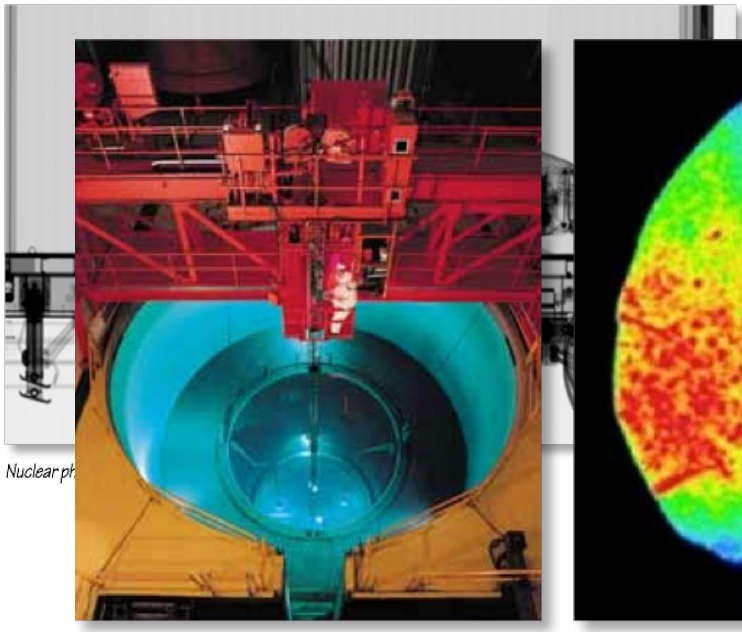

Nuclear ph

Next-generation nuclear reactors will operate with increased safety and flexibility.

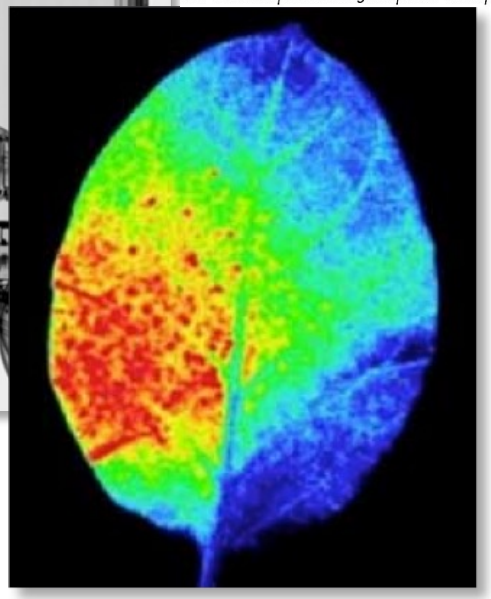

PET scans reveal how plants respond to rising CO_2.

Archaeologists used accelerator-based studies to more accurately date 12,000-year-old cave paintings.